AGE OF INFORMATION-ORIENTED COMPARATIVE EVALUATION OF CHANNEL ACCESS MECHANISMS IN MULTI-RATE WIRELESS LANS

A THESIS SUBMITTED TO
THE GRADUATE SCHOOL OF ENGINEERING AND SCIENCE
OF BILKENT UNIVERSITY
IN PARTIAL FULFILLMENT OF THE REQUIREMENTS FOR
THE DEGREE OF
MASTER OF SCIENCE
IN
ELECTRICAL AND ELECTRONICS ENGINEERING

By
Umut Utku Erdem
August 2023

Age of Information-oriented Comparative Evaluation of Channel Access Mechanisms in Multi-rate Wireless LANs
By Umut Utku Erdem
August 2023

We certify that we have read this thesis and that in our opinion it is fully adequate, in scope and in quality, as a thesis for the degree of Master of Science.

Ezhan Karaşan(Advisor)

Nail Akar(Co-Advisor)

Elif Tuğçe Ceran Arslan

Mehmet Akif Yazıcı

Approved for the Graduate School of Engineering and Science:

Orhan Arıkan
Director of the Graduate School

ABSTRACT

AGE OF INFORMATION-ORIENTED COMPARATIVE EVALUATION OF CHANNEL ACCESS MECHANISMS IN MULTI-RATE WIRELESS LANS

Umut Utku Erdem
M.S. in Electrical and Electronics Engineering
Advisor: Ezhan Karaşan
August 2023

Delay-sensitive applications have recently garnered significant attention because of the increasing demand for real-time data and time-critical information. In delay-sensitive systems, the timeliness of the delivered information is crucial to guarantee a reliable operation. A performance metric called Age of Information (AoI) is introduced in the literature to measure the freshness of information. In this study, various channel access methods are comparatively evaluated for stations transmitting age-sensitive status update packets over a multi-rate IEEE 802.11 WLAN. For wireless networks carrying conventional data traffic, the legacy channel access mechanism imposed by the Distributed Coordination Function (DCF) allows sources to access the channel equally. This mechanism results in a throughput-fair bandwidth allocation which is also known as a performance anomaly in the literature. Airtime-fair channel access methods have been proposed in the literature for multi-rate wireless LANs to mitigate this anomaly. Recently, there has been a surge of interest in status update systems with the emergence of performance criteria called age of information. Age-based performance metrics (AoI, peak AoI) are more effective to satisfy the requirements of the carried age-sensitive traffic as opposed to using conventional performance metrics (throughput, delay, or loss). In this study, we propose a novel channel access mechanism for age-sensitive traffic which is devised to lessen the mean Peak AoI (PAoI) averaged over all the sources in the network, which is termed as the system PAoI. The proposed channel access mechanism effectively reduces the system PAoI compared to LCA and PFCA. Although system PAoI performance improvement depends on the system configuration, i.e. packet size, the multi-rate mixture of the network etc., system PAoI can be reduced up to 12.04% and 27.44% compared to the legacy channel access and airtime-fair channel access, respectively, for the considered system configurations in this study. Although the

proposed channel access mechanism outperforms legacy and airtime-fair channel access mechanisms in terms of system PAoI, it may lead to a reduction in the overall throughput of the system compared to airtime-fair channel access.

Keywords: Status update systems, Age of Information, Peak Age of Information, IEEE 802.11 Distributed Coordination Function, Airtime fairness.

ÖZET

ÇOKLU-HIZLI KABLOSUZ YEREL AĞLARDA KANAL ERİŞİM MEKANİZMALARININ BİLGİNİN YAŞI ODAKLI KARŞILAŞTIRILMASININ DEĞERLENDİRMESİ

Umut Utku Erdem
Elektrik ve Elektronik Mühendisliği, Yüksek Lisans
Tez Danışmanı: Ezhan Karaşan
Ağustos 2023

Gecikmeye duyarlı uygulamalar, gerçek zamanlı verilere ve zaman açısından kritik bilgilere yönelik artan talep nedeniyle son zamanlarda önemli bir ilgi görmektedir. Gecikmeye duyarlı sistemlerde, iletilen bilginin güncelliği güvenilir çalışmayı garanti etmek için çok önemlidir. Bilginin tazeliğini ölçmek için literatürde bilgi yaşı adı verilen bir performans ölçütü tanıtılmıştır. Bu tez çalışmasında, çoklu-hızlı IEEE 802.11 kablosuz LAN üzerinde yaşa duyarlı durum güncelleme paketleri ileten istasyonlar için kanal erişim yöntemleri incelenmiştir. Geleneksel veri trafiği taşıyan kablosuz ağlar için, Dağıtılmış Koordinasyon Forksiyonu (DCF) tarafından tanımlanan geleneksel kanal erişim mekanizması, istasyonların kanala eşit şekilde erişmesine izin vermektedir. Geleneksel kanal erişim mekanizması, çoklu-hızlı ağlarda kullanıcılar arasında veri hacmi-adil bant genişliği tahsisi yaparak literatürde de iyi bilinen performans anomalisine yol açmaktadır. Bu anomaliyi düzeltmek için, literatürde hava-zaman-adil kanal erişim yöntemleri önerilmiştir. Son zamanlarda, bilginin yaşı gibi performans ölçütlerinin de çıkmasıyla birlikte durum güncelleme sistemlerine olan ilgi artmıştır. Bu sistemlerde taşınan yaşa duyarlı trafiğin gereksinimlerini karşılamak için veri hacmi, gecikme, kayıp gibi geleneksel performans ölçütleri yerine bilgi yaşı (AoI), tepe bilgi yaşı (PAoI) gibi ölçütlerin daha etkili olduğu görülmüştür. Bu çalışmada, ağdaki kanala erişmek için yarışan kaynakların tepe bilgi yaş değerlerinin ortalaması alınmış ortalama tepe bilgi yaşını (PAoI) düşürmek üzere tasarlanmış yeni bir kanal erişim mekanizması önerilmiştir. Sistemin ortalama tepe bilgi yaşı sistem PAoI olarak adlandırılmıştır. Önerilen erişim mekanizması, diğer erişim mekanizmalarına kıyasla, sistem PAoI parametresini efektif bir

şekilde düşürmektedir. Yüzdesel olarak iyileşme miktarı gözönünde bulundurulan sistemin koşullarına, örneğin paket boyutu, istasyonların hız dağılımı, istasyon sayısı gibi, bağlıdır ancak bu çalışmada değerlendirilen sistem koşullarında sistem PAoI parametresinde geleneksel kanal erişim mekanizmasına kıyasla 12.04%, hava-zaman-adil kanal erişim mekanizmasına kıyasla 27.44% iyileşme gözlenmiştir. Önerilen erişim mekanizması diğer erişim mekanizmalarına karşı sistem PAoI açısından daha iyi performans göstermesine karşın hava-zaman-adil kanal erişim mekanizmasına kıyasla sistemin toplam veri hacminin düşmesine yol açabilmektedir.

Anahtar sözcükler: Durum güncelleme sistemleri, bilgi yaşı, tepe bilgi yaşı, IEEE 802.11 Dağıtılmış Koordinasyon Fonksiyonu, yayın zamanı adaleti.

Acknowledgement

I would like to thank Prof. Dr. Ezhan Karaşan and Prof. Dr. Nail Akar for their valuable guidance, patience, time, and continuous support throughout this study. Working with them was a great pleasure and experience for me. I would like to thank Assist. Prof. Elif Tuğçe Ceran Arslan and Dr. Mehmet Akif Yazıcı for agreeing to be on my thesis committee. I would also like to thank my family members, my wife Aysu, my mother Sevinç, my father Ayhan, and my sister Bensu for their continuous support and encouragement throughout my study.

Contents

List of Figures

List of Tables

Chapter 1

Introduction

1.1 Overview

Recently, low latency system applications including autonomous vehicles, Industry 4.0, remote surgery operations, etc., are getting noticed significantly with the advancements in information technology. In these system applications, generated time-stamped status update messages at the source are transmitted through a network to the monitoring system. Timely delivery of the information is crucial for these real-time applications. The concept of age of information (AoI) was introduced in [2] to measure the freshness of data at the monitor. The AoI process for a source amounts to the measured elapsed time at the monitor since the generation of the last successively received update packet. In AoI system models, the main objective of the monitor is to possess the most up-to-date status update packet. Hence, mechanisms and tools are necessary to keep the weighted sum of the mean AoI of sources as small as possible. However, obtaining and optimizing analytical expressions for mean AoI in certain cases is known to be a challenging problem. Even in basic scenarios, minimizing the age of information in a monitoring system with multiple sources is not a simple task.

Calculating average age analytically is generally known to be a challenging

problem, since average-time age depends on the expected value of multiplication of system time (T_n) and inter-arrival time (Y_n) for stationary and ergodic (Y_n, T_n) process, where the system time and inter-arrival time are negatively correlated [3],[4]. Therefore, an alternative metric called peak AoI, which indicates the maximum age that is reached right before receiving a status update packet, is introduced in [5]. By using PAoI as a performance metric, the computation of $\mathbb{E}[T_n Y_n]$ is avoided for calculating average age statistics [3]. Closed-from expressions are available for mean PAoI which are suitable for optimization [6]. Also, in certain systems, we may want to have the system such that the peak age stays under a threshold with a certain probability. Hence, designing a system based on the peak AoI is of interest.

Our study is based on the IEEE 802.11 [1] standard that defines MAC and PHY protocols for a WLAN with an Access Point (AP) and multiple stations. There are two access techniques defined in the IEEE 802.11 standard: Point Coordination Function (PCF) and Distributed Coordination Function (DCF).

PCF is a polling-based contention-free MAC protocol that uses a centralized mechanism to access the channel. When operating in PCF, AP acts as the point coordinator (PC), and the time slots are allocated by the PC to the stations in the network to transmit its packet. A beacon frame is periodically broadcasted by the PC to initiate the Contention-Free Period (CFP) and provide information to the stations about the duration of the CFP. During the CFP, each station in the network waits to be polled by AP to initiate the data transmission through the channel. The station list is maintained at the AP and polling is applied according to round-robin fashion. Air-time fairness can be provided among different stations by providing equal air times in a multi-rate PCF network. PCF and DCF mechanisms can coexist by dividing the beacon interval into Contention Free Period (CFP) and Contention Period (CP) which uses the PCF and DCF channel access mechanisms, respectively. PCF is an optional MAC protocol that is defined in the IEEE 802.11 standard and it is not widely implemented in the telecommunications industry which is not the scope of this study.

Our study is based on the DCF mechanism defined in the IEEE 802.11 standard [1]. We use the Carrier Sense Multiple Access with Collision Avoidance (CSMA/CA) access mechanism in our study to manage contention among the stations in the wireless network. In CSMA/CA, at first, each station with a frame in its queue senses the channel to start the transmission process. If the channel is sensed as busy, the station waits until the channel becomes idle, then waits for a specified Distributed Inter-frame Space (DIFS) before initiating a random binary exponential backoff process. During the backoff process, which is used for collision avoidance purposes, the station waits for a random number of slots uniformly chosen between 0 and $CW-1$ where the Contention Window (CW) is set to minimum contention window size (CW_{min}) for the first transmission attempt before starting the transmission. When a collision occurs, CW size is doubled until the maximum contention window size (CW_{max}) is reached. Collision probability due to multiple nodes transmitting simultaneously on a shared channel is decreased thanks to the exponential backoff mechanism in CSMA/CA. When the backoff timer is down to zero, the station transmits its packet to the Access Point (AP) and waits for an Acknowledgement (ACK) message. If an ACK message is not received during a specified ACK timeout duration, the message is considered to be dropped and the retransmission process starts.

There can be scenarios that station evaluates the channel as idle, although there is an ongoing transmission from an out-of-range station to the AP in CSMA/CA channel access mechanism. This problem is called as hidden terminal problem in the literature and an optional 4-way handshake procedure known as Request-to-Send/Clear-to-Send (RTS/CTS) mechanism is proposed in the standard to overcome hidden terminal problem [1]. In RTS/CTS mechanism, the station, which wants to transmit, sends an RTS message to AP and AP replies to this request by sending a CTS message which contains the information about reservation duration. CTS message is received by all stations that are in the range of AP and the hidden terminal problem is solved thanks to the RTS/CTS mechanism. However, the 4-way handshake procedure is not considered in this study and a basic CSMA/CA based DCF mechanism is used.

In the IEEE 802.11 WLANs, some stations might be located far away from

the AP and this results in a decrease in the received signal quality. In these situations, the station needs to operate at lower data rates based on the received signal level from AP, resulting in a multi-rate WLAN. In multi-rate WLANs, we term the channel access mechanism, where all of the stations use the same set of parameters, e.g. CW_{min}, as the Legacy Channel Access (LCA). Long-term channel access probabilities are equal for all sources in LCA, and this results in throughput-fair bandwidth allocation for identical average frame sizes across all stations. In LCA, when there is even a single low-rate station in a multi-rate wireless network, the overall performance of the network in terms of throughput is significantly decreased. This phenomenon is explained in reference [7] and it is known as the performance anomaly problem in the literature. This anomaly results from long-term equal channel access probabilities between stations with different transmission rates.

Airtime fairness is proposed in the literature as an alternative to throughput fairness to solve the performance anomaly by allocating wireless channels to competing stations with equal amounts of airtime usage. By using airtime fairness, the throughput of a station ends up being proportional to its transmission rate, guaranteeing that stations with low data rates will no longer drag down stations with high data rates [8]. On the contrary, proportional fair resource allocation maximizes the sum of the logarithms of user throughputs to provide a balance between efficiency and fairness [9]. Equality of airtime fairness and proportional fairness for wireless networks was presented in [8]. Additionally, it has been presented in [10] that the throughput of a station is inversely proportional to its CW_{min} parameter in IEEE 802.11 DCF WLANs. Hence, airtime fairness can be approximately achieved by selecting the initial contention window size CW_{min} of a station as inversely proportional to the transmission rate of the station, which is termed as Proportional-Fair Channel Access (PFCA) in this study. Existing LCA and PFCA mechanisms do not consider age-based performance metrics. In this study, we propose a novel channel access mechanism with the goal of reducing system PAoI in IEEE 802.11 DCF multi-rate WLANs by solving an analytical model for the mean Peak AoI of the network. The proposed model is denoted as the System PAoI-based Channel Access (SPCA) mechanism and the CW_{min}

parameter of each station should be selected to be inversely proportional with the square root of the transmission rate in contrast to the PFCA mechanism.

1.2 Thesis Contributions

The main contribution of this thesis is the development of a system PAoI-based simple yet effective channel access mechanism with the goal of minimizing system PAoI in multi-rate IEEE 802.11 DCF WLANs, which is called System PAoI-based Channel Access (SPCA). We provide an analytical framework for the justification of why SPCA minimizes system PAoI. Existing throughput fair LCA and airtime fair PFCA mechanisms, which are used in IEEE 802.11 DCF WLANs, are evaluated using simulations and compared with the proposed mechanism in terms of system PAoI, system AoI, and throughput in this study. Although the proposed SPCA mechanism, outperforms LCA and PFCA mechanisms in terms of system PAoI, it may reduce total throughput compared to the air-time fair mechanism.

1.3 Thesis Outline

This thesis is organized as follows. The literature review is given in Chapter 2. In Chapter 3, we clarify the system model by describing the considered model that is used and formulating the optimization problem. We express the channel access probability of each mechanism analytically. In Chapter 4, we explain 3 different channel access mechanisms of interest in detail, namely LCA, PFCA, and SPCA. Chapter 5 presents numerical results for comparative evaluation of channel access mechanisms in terms of system PAoI, system AoI, and throughput that are obtained by using Python-based IEEE 802.11a DCF simulator [11]. Additionally, optimal minimum contention window pair is found for a network where the station's data rates are from 2 classes in Chapter 5. A slight deviation is observed from the optimal point when the proposed model is used and the reason is explained. Chapter 6 presents the conclusions and future works.

Chapter 2

Literature Review

2.1 Age-oriented Scheduling Mechanisms

AoI- or PAoI-aware scheduling mechanisms have been studied for coordinated access networks in the literature. An optimal joint sampler-scheduler pairs are proposed in reference [12], to minimize the total-average age-penalty (TA-AP) and the total-average age-penalty at delivery times (TA-APD) for multi-source coordinated access network. It is presented that Maximum Age First (MAF) scheduling policy, for which the source with the greatest age is prioritized and served first, is the optimal scheduler to minimize both TA-AP and TA-APD. Different scheduling policies are proposed for symmetric and asymmetric wireless networks in [13], where a system model with broadcast transmission of age-sensitive traffic from the server (base station) to multiple nodes is considered. It is shown in [13] that proposed Greedy, Max-weight, and Whittle index policies are the optimal scheduling policies for symmetric networks to minimize the mean weighted sum AoI of all nodes. For asymmetric networks, strong performances of Max-weight and Whittle index policies are presented in [13].

Despite the existence of numerous studies about scheduling mechanisms in coordinated access, there has been far less working literature on different random

access channels. Age-dependent random access mechanism is proposed in the reference [14] for large-scale networks (IoT). Eligibility of transmission is decided according to the threshold, i.e. only stations whose age exceeds the threshold can access the channel. Also, equal channel access probability is assigned to stations that meet the threshold criteria. Reference [15] proposes a variation of ALOHA, called threshold-ALOHA (TA), a distributed age-aware modification of slotted ALOHA for which each station suspends its transmissions until the AoI reaches a certain threshold for ALOHA-type random access mechanism. In [16], a modified version of the slotted ALOHA, called Minislotted Threshold ALOHA (MiSTA), is proposed to minimize the mean AoI in the network. Like in [15], sources become active when they reach a certain threshold in [16]. In MiSTA, the short control sequence is transmitted in a minislot before the actual data transmission which provides collision detection and channel sensing. The performance improvement of MiSTA over TA is demonstrated in [16]. Modern random access protocol, called Irregular Repetition Slotted ALOHA (IRSA) which is proposed in [17], is investigated in terms of Age of Information in [18]. Essentially, in the IRSA protocol, the source transmits multiple replicas of its status update messages in randomly selected slots in a frame. The closed-form expressions for age violation probability and mean AoI in IRSA protocol are presented in [18]. Additionally, the superior performance of IRSA over Slotted ALOHA is highlighted in [18]. In [19], Age-critical Frameless ALOHA (ACFA) random access protocol is proposed. Fundamentally, the mean AoI is decreased by banning the transmission of active sources recovered successfully in the last frame. Theoretical analysis and simulation results are demonstrated in [19] to support the findings in both dense and sparse access models. In [20], analytic models for the V2X standard IEEE 802.11p for AoI are proposed. In [21], AoI in the CSMA environment is investigated for the scenario where N stations contend for channel. A closed-form expression for the system's total AoI is derived as a function of average transmission time, average backoff time, and arrival rate using Stochastic Hybrid Systems [22] for generate-at-will and stochastic packet arrival policies. In [21], to minimize total AoI in the network, the optimization problem is formulated and solved to find the backoff time of each station that minimizes total AoI. Although collisions are not taken into account in [21], collision effects in random access mechanisms are

considered in [23], where approximate expressions of mean AoI are presented for slotted ALOHA and CSMA by using a discrete-time model. As there has been less work on IEEE 802.11 DCF CSMA/CA based networks in the AoI literature, there is still a need for the development of practical channel access mechanisms for IEEE 802.11 wireless networks, which is the scope of this study. Also, in this study, our main motivation is to reduce system Peak AoI in the CSMA/CA environment although we have investigated the performance of the proposed method in terms of system AoI.

2.2 AoI Optimization using Learning Models

There are some recent studies that use learning models to minimize AoI. A network with sensors in which each sensor transmits its status update packets to the remote monitoring system is considered in [24]. The goal of the study is to optimize the weighted sum of average AoI by minimizing the probability of exceeding a certain age threshold for each sensor. A Reinforcement Learning (RL) based algorithm is used to select which sensor to transmit. In [25], Q-learning and policy gradient methods are used in a multi-queue system model with a single server, and an AoI-optimal scheduler is proposed. These models are compared with the MAF scheduler. In [26], the optimal update rate is adjusted which minimizes AoI throughout the WiFi network by using the Deep Learning model. An alternative model to the learning-based model is proposed by the same authors in [27], which is an iterative method proposed to find an optimal arrival rate that reaches the target offered load ρ^*, and minimizes AoI for the remote monitoring system. In [27] and [26], the service rate of the physical layer μ, is calculated by only using the probability of collision which is simply calculated by using RTS message statistics. The optimal arrival rate is iteratively adjusted in the MAC queue by considering the service rate of the physical layer to minimize AoI.

2.3 Performance Anomaly in the IEEE 802.11 WLANs and Airtime Fairness

For IEEE 802.11 DCF-based multi-rate WLANs, using the basic CSMA/CA mechanism with the same parameter set such as CW_{min} results in equal long-term channel access probabilities between the sources and provides throughput fairness among stations. However, low-rate stations occupy channel more than high-rate stations when equal packet size is considered at each station, and this causes significant deterioration in the total throughput of the network and this is called as performance anomaly in the literature [7]. Instead of using a throughput fair access mechanism which results in performance anomaly, alternative airtime fair access mechanisms can be used [28], [29]. By providing equal air time-share to competing stations, performance anomaly can be cleanly solved. With air-time fairness, the throughput of a station turns out to be proportional to its data rate ensuring that slow-rate stations will no longer drag down the faster stations [29]. On the other hand, proportional fair resource allocation provides a balance between fairness and efficiency through the maximization of the sum of the logarithms of user throughput [9]. In [8], it is shown that proportional fairness and airtime fairness are equivalent for wireless LANs. The references [10] and [30] analytically prove that the throughput of an individual station is inversely proportional with the CW_{min} value of the station for DCF under certain assumptions. An alternative distributed air-time fair channel access mechanism is proposed in [31] by keeping the conventional DCF operation that is defined in the IEEE 802.11 standard. Airtime fairness is provided in [31] by using the proposed airtime fair MAC protocol, called Multiple DCF (MDCF), which is mainly based on running several backoff processes at each station. In [32], an idle sense access mechanism is proposed to select CW_{min}, in which each node adjusts its contention window by estimating the number of idle slots between two consecutive transmission attempts for the modified version of basic CSMA/CA without the exponential backoff mechanism. In [32], minimum contention windows are scaled based on data rates for multi-rate networks. In [33], it is presented that using data rates for contention window scaling as in [32] and [10] has several

drawbacks. An alternative Time Fair Carrier Sense Multiple Access (TFCSMA) protocol is proposed in which the minimum contention window of stations is adjusted by using a distributed online algorithm to have a long-term airtime fair system.

Chapter 3

System Model

3.1 Model Description

We consider a system with multiple information sources, i.e., $s_i,\ i = 1, 2, \ldots, N$, each of which samples a source-specific stochastic process $Y_i(t)$ at certain times and places the samples and sampling times in the status update packets which are then transmitted to a remote monitoring system through a multi-rate IEEE 802.11 WLAN. At a given transmission opportunity, a source can freely select one of the standard transmission rates according to the channel conditions in multi-rate WLANs which is referred to as the link adaptation feature. In our system model, we assume that all the information packets have the same size B for all the sources. Moreover, we assume that the transmission times from the Access Point (AP) to the remote monitor are negligible thanks to the AP and remote monitor either being connected via a high-speed link or co-located. Basic CSMA/CA with binary exponential backoff and without RTS/CTS mechanism is used as a channel access mechanism which is known as the Distributed Coordination Function (DCF) and mandatory in the IEEE 802.11 standard [1]. We assume that all stations are in a saturated state, i.e., always have packets to transmit, and, waiting packet is preempted by fresh arrival at the queues. For

all the sources, we employ the generate-at-will model in which the source processes are sampled only at the transmission opportunities decided by the DCF. The process for a specific source, say s_i, is described as follows. Source s_i firstly senses the channel to detect an idle duration of at least equal to the Distributed Inter-Frame Space (DIFS). Immediately afterward, s_ℓ sets its backoff timer value to a number that is selected uniformly from the interval $[0, CW_{min,i} - 1]$ where $CW_{min,i}$ denotes the minimum contention window size for s_i. The backoff timer for s_i is then decremented at each slot boundary as long as there is no ongoing transmission on the channel, i.e., idle. On the other hand, the backoff timer is stopped when a transmission is detected on the channel which results from any other source in the network. When the channel is sensed as idle for at least DIFS duration, the backoff timer continues the countdown. When the backoff timer hits zero, s_i has the transmission opportunity at which it samples the process $Y_i(t)$ and forms the status update packet in line with the generate-at-will model and starts transmitting its information packet. We assume that sampling the process $Y_i(t)$ and forming the packet is instantaneous. When the AP successfully receives the transmitted information packet, it sends an acknowledgment message (ACK) after waiting a short inter-frame space (SIFS) duration. When the transmission opportunities of multiple sources coincide, then a collision takes place. The source s_i acknowledges the collision cases if it does not receive an ACK during a specified ACK timeout duration. The contention window size is doubled after each unsuccessful transmission attempt which starts from initial contention window size $CW_{min,i}$, until maximum contention window size CW_{max} is reached. When a packet successfully send or the retransmission limit is exceeded, the contention window size is decreased to $CW_{min,i}$ and the process is repeated for the sequential information packet. We assume that packet transmission errors only happen because of collisions and channel errors are neglected in this study. Additionally, we assume that stationary sources throughout the network and we assign a fixed transmission rate to each station. The basic system model and age processes of source s_i are shown in Fig. 3.1 for an example scenario.

In Fig. 3.1, T_i denotes the transmission time of status update packets for source s_i. Fig. 3.1 shows a sample path of the AoI process $A_i(t)$ associated with s_i for

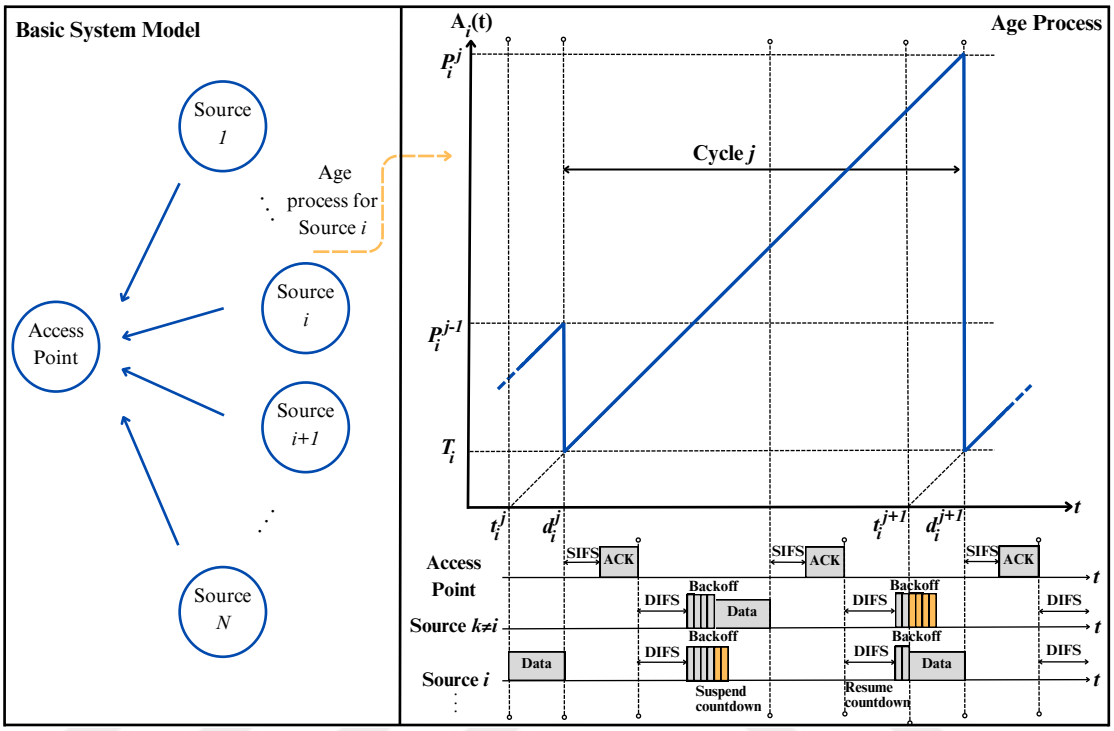

Figure 3.1: Basic System Model

cycle-j during which $A_i(t)$ increases with unit slope from the value T_i at d_i^j until time d_i^{j+1}. At the beginning of the sample path presented in Fig. 3.1, it is assumed that the source s_i has already passed its backoff process and starts its successful data transmission for packet j at time t_i^j and there are no other stations that start data transmission at the same time instance. Immediately afterward, the monitor receives the transmitted information packet (data) at time d_i^j at which instance the AoI process instantly drops to T_i. Subsequently, the AP then for a SIFS duration and sends an ACK message to s_i. Afterward, all sources wait for the channel to become idle for a DIFS duration and s_i starts its backoff process. At this moment, the source $s_k, k \neq i$ has the minimum remaining backoff value in terms of slots (four in this example) among the other stations. Therefore, source s_k gets the channel after waiting for four slots at which instance the source s_i freezes its backoff timer, suspends its countdown (2 slots remaining), and waits for the channel to be idle for a DIFS duration. After that, information packet (data) transmission of s_k starts and all sources which are in the backoff process freeze their timers. Hence, the AoI process $A_i(t)$ in Fig. 3.1 is associated with

s_i, received data at the AP from source s_k does not affect the AoI process of source s_i, $A_i(t)$. Subsequently, the AP waits for a duration of SIFS and sends its ACK message to source s_k. At the following contention, stations that freeze their timers during the previous contention period, resume their countdown processes. At this point, s_i has the minimum number of remaining slots among all contending stations. After the duration of two slots, s_i sends its data at t_i^{j+1}. When data is received by the AP at d_i^{j+1}, the AoI process for s_i again suddenly drops to the value T_i. When backoff timers of two or more stations hit zero at the same time instance, collision happens due to multiple transmissions at this instance. However, the sample path shown in Fig. 3.1 for example scenario is envisioned to be collision-free. As shown in Fig. 3.1, the AoI process increases with unit slope during cycle j from the value T_i at t_i^j until time t_i^{j+1}. On the other hand, the PAoI process P_i^j is obtained by sampling the AoI process just before the reception instance of packet $j+1$. The steady-state values of the AoI and PAoI processes of s_i are denoted by A_i and P_i, respectively. We denote the weighted system PAoI, P_w, which is the weighted average of the mean PAoI of the sources and it can be calculated as:

$$P = \sum_{i=1}^{N} \mathbb{E}[P_i] w_i, \tag{3.1}$$

consequently the weighted system AoI, A_w can be obtained as:

$$A = \sum_{i=1}^{N} \mathbb{E}[A_i] w_i, \tag{3.2}$$

In our study, we assume equal weights across the information sources which leads to $w_i = 1/N$. Therefore, system PAoI P can be calculated as:

$$P = \frac{1}{N} \sum_{i=1}^{N} \mathbb{E}[P_i], \tag{3.3}$$

3.2 Optimization Problem Formulation

As the performance metric of interest, we will employ the system PAoI and system AoI in which the system PAoI is suitable for optimization [6]. On the other hand,

optimization of system AoI is left for future research. However, simulation results for both of the age metrics will be shared in Chapter 5. As shown in Fig. 3.1, P_i^j can be calculated by adding two service times of successively scheduled s_i information packets and the sum of the Z_i^j and I_i^j, where the random variable Z_i^j denotes the total service time of all the packets successfully transmitted from sources $k \neq i$ during the cycle j. Whereas, the random variable I_i^j represents the elapsed time that is not used for successful transmissions, i.e., collisions, protocol overheads, transmission of ACK messages, etc., during cycle j. The time interval $(t_i^{j+1} - d_i^j)$ shown in Fig. 3, consists of summation of the Z_i^j and I_i^j components. In this study, τ_i denotes the long-term fraction of time that the channel is used by s_i for successful transmission. The channel utilization of the entire system, overall utilization of the channel, can be simply calculated by adding up τ_i of all sources in the network, i.e.,

$$\tau = \sum_{i=1}^{N} \tau_i \tag{3.4}$$

It can be clearly seen that the overall utilization of the channel is always less than 1 for the considered system model because of nonzero I_i^j components. Additionally, overall utilization of the channel depends on several parameters such as the number of stations in the network N, the packet transmission time of each source T_i, and IEEE 802.11 protocol parameters such as minimum contention window size $CW_{min,i}$ and retransmission limit r_i.

One can easily write the mean PAoI for source s_i as follows,

$$\mathbb{E}[P_i] = 2T_i + \mathbb{E}[I_i] + \mathbb{E}[Z_i] \tag{3.5}$$

By observing the cycle j of the sample path in Fig. 3.1, the channel utilization parameter τ_i can be written as,

$$\tau_i = \frac{T_i}{T_i + \mathbb{E}[Z_i] + \mathbb{E}[I_i]} \tag{3.6}$$

The following closed-form expression for the mean Peak AoI of source s_i can be obtained in terms of τ_i,

$$\mathbb{E}[P_i] = \left(1 + \frac{1}{\tau_i}\right) T_i \tag{3.7}$$

Let w_i denote the weight of source s_i. Therefore, the weighted system PAoI P_w can be written as a function of the weight of source s_i and utilization parameters $\tau_i, i = 1, \ldots, N$, as follows,

$$P_w = \sum_{i=1}^{N} \left(1 + \frac{1}{\tau_i}\right) w_i T_i. \tag{3.8}$$

The main purpose of this study is to propose a mechanism that minimizes P_w. We denote the probability of a successful transmission on the channel belonging to source s_i is denoted as p_i. We know that τ_i is proportional with the $p_i T_i$ expression where $\sum_{i=1}^{N} p_i = 1$. Therefore, one can write p_i in terms of τ_i as follows,

$$p_i = \frac{\tau_i / T_i}{\sum_{j=1}^{N} \tau_j / T_j} \tag{3.9}$$

Contrarily, one can write τ_i in terms of p_i and the overall utilization parameter τ as follows,

$$\tau_i = \tau \frac{p_i T_i}{\sum_{j=1}^{N} p_j T_j} \tag{3.10}$$

As a result, firstly, the channel utilization parameters can be found according to (3.10) for given channel access probabilities p_i and τ, which then leads to the expressions for per-source mean PAoI values and weighted system PAoI in (3.7) and (3.8), respectively. The parameter τ is not known in advance. Nevertheless, it can be approximately obtained by analytical methods when the protocol and traffic parameters are given.

A similar generate-at-will system model with N sources and without packet errors for a coordinated access mechanism is considered in [6], where the server decides which source to sample, form, and transmit its information packets at each scheduling instant. After each transmission, the server schedules the transmission of a new information packet. In [6], two schedulers are proposed which are named the Weighted Proportional Fair Scheduler (WPFS), and the Weighted Sum Peak AoI Scheduler (WSPS), where the former maximizes the sum of the logarithms of source throughputs and the latter minimizes the weighted sum peak AoI of all

sources. It is clear that the overall utilization of the system is 1 for this scenario and the long-term fraction of time that the link is utilized to transmit packets from source i, denoted by τ_i should be equal to the weight of s_i for achieving proportional fairness for WPFS [6]. This leads to the selection of $p_i \propto w_i/T_i$ where p_i, w_i, and T_i denote the long-term frequency of packet transmissions from source s_i, the weight, and the mean service duration of source s_i, respectively. On the other hand, the p_i parameter for each source should be adjusted according to the $p_i \propto \sqrt{w_i/T_i}$ rule to minimize the sum PAoI for WSPS [6]. Although the system model in [6] does not include a random access mechanism, the convex optimization problem turns out to be the same for the IEEE 802.11 wireless LAN scenario for a fixed channel utilization of the entire system τ. In [6], the optimization problem with equation (3.8) subject to $\tau = 1$ is solved, and p_i parameters that minimize the equation (3.8) are calculated. The system model in [6] is error-free which leads to $\tau = 1$. However, in our system model, τ is less than one due to collisions and protocol overheads. On the other hand, by assuming a fixed overall utilization for the system, we can solve the same convex optimization problem in (3.8) in a similar way. The steps for the solution of the optimization problem are provided in Chapter 4. Additionally, we solve the convex optimization problem by considering different weights across the sources. On the other hand, we used equal weights across the information sources for the considered channel access mechanisms and simulations.

Chapter 4

Channel Access Mechanisms

There are several distributed channel access mechanisms in the literature for the IEEE 802.11 DCF WLANs. Throughput-fair Legacy Channel Access (LCA), airtime-fair Proportional-Fair Channel Access (PFCA), and the proposed System PAoI-based Channel Access mechanisms are explained in this chapter. Solution for the optimization problem stated in Section 3.2 is provided in Section 4.3.

4.1 Legacy Channel Access (LCA) Mechanism

Different channel access algorithms select the channel access probabilities in different ways. In Legacy Channel Access (LCA), DCF parameters for all the sources are equal and therefore channel access probabilities are identical for all sources [7],

$$p_i = \frac{1}{N},\ 1 \leq i \leq N. \tag{4.1}$$

However, identical channel access probabilities results in well-known performance anomaly problem in the IEEE 802.11 WLANs. Therefore, alternative channel access mechanisms are provided in the literature, and the airtime fair access mechanism is explained in the next section.

4.2 Proportional Fair Channel Access (PFCA) Mechanism

In the Proportional Fair Channel Access (PFCA) mechanism, $\tau_i = w_i$ when we consider a weighted system model. Under the assumption of equal weights, PFCA, also known as Airtime Fair CA (AFCA), channel utilization of each source is equal [8], i.e.,

$$\tau_i = \tau_j, 1 \leq i, j \leq N, \tag{4.2}$$

which leads to the following closed-form expression for the channel access probabilities

$$p_i = \frac{1/T_i}{\sum_{j=1}^{N} 1/T_j}, \tag{4.3}$$

Therefore, the channel access probability of each station is selected as inversely proportional to its transmission time for PFCA. An easy way to do this is to adjust the DCF parameter of each source which will be explained in Section 4.4.

4.3 System PAoI-based Channel Access (SPCA) Mechanism

In this study, we propose a novel channel access mechanism for age-sensitive traffic to reduce the system Peak PAoI which we term as System PAoI-based Channel Access (SPCA). The minimization problem of the weighted system PAoI P_w in (3.8) in terms of the optimization variables $\tau_i,\ 1 \leq i \leq N$, subject to $\sum_{i=1}^{N} \tau_i = \tau,\ \tau_i \geq 0$, is a convex optimization problem for which the Karush-Kuhn-Tucker (KKT) conditions are necessary and sufficient [34]. To observe this, one can consider a convex function of $\frac{1}{y}$ where $y > 0$. For non-negative weights, the sum of convex functions is also convex. The steps for the optimization process

are as follows,

$$\nabla P_w(\tau_1, \tau_2, \ldots, \tau_N) = \begin{bmatrix} -\frac{w_1 T_1}{\tau_1^2} \\ -\frac{w_2 T_2}{\tau_2^2} \\ \vdots \\ -\frac{w_N T_N}{\tau_N^2} \end{bmatrix} \tag{4.4}$$

Let $g(\tau_1, \tau_2, \ldots, \tau_N) = \sum_{i=1}^{N} \tau_i$. The gradient of the function g can be calculated as,

$$\nabla g(\tau_1, \tau_2, \ldots, \tau_N) = \begin{bmatrix} 1 \\ 1 \\ \vdots \\ 1 \end{bmatrix} \tag{4.5}$$

To find the minimum point, we can use Lagrange multiplication and equate the expression to zero.

$$\nabla P_w - \lambda \nabla g = \begin{bmatrix} -\frac{w_1 T_1}{\tau_1^2} - \lambda \\ -\frac{w_2 T_2}{\tau_2^2} - \lambda \\ \vdots \\ -\frac{w_N T_N}{\tau_N^2} - \lambda \end{bmatrix} = \begin{bmatrix} 0 \\ 0 \\ \vdots \\ 0 \end{bmatrix} \tag{4.6}$$

By using the N equations given in (4.6), and $\sum_{i=1}^{N} \tau_i = \tau$, we can write λ as follows,

$$\lambda = \frac{1}{\tau^2} \left(\sum_{i=1}^{N} \sqrt{w_i T_i} \right)^2 \tag{4.7}$$

By using expressions given in (4.6) and (4.7), we can find τ_i of each source that minimizes the weighted system PAoI for fixed overall utilization. Therefore, the weighted system PAoI P_w can be minimized for a fixed overall utilization with the selection of the channel utilization parameters τ_i as follows,

$$\tau_i = \tau \frac{\sqrt{w_i T_i}}{\sum_{j=1}^{N} \sqrt{w_j T_j}}, \quad 1 \leq i \leq N. \tag{4.8}$$

Under the assumption of equal weights across sources, which leads to a choice of $w_i = 1/N$ the channel access probabilities p_i that minimize the system PAoI can

explicitly be given as,

$$p_i = \frac{\sqrt{1/T_i}}{\sum_{j=1}^{N} \sqrt{1/T_j}}, \tag{4.9}$$

without dependence on the channel utilization parameter τ which may not be known accurately in advance. DCF parameter minimum contention window size can be modified to adjust per-source channel access probabilities. The following section will explain the scaling policies for each access mechanism.

4.4 Distributed Scaling Policies for Airtime Fairness

Adjusting the per-source DCF parameters so that different channel access probabilities are attained is a well-studied problem in the literature [10], [32], [33]. The most widely used such method adjusts the DCF parameter $CW_{min,i}$ on the basis of the observation that individual throughput attained by source s_i is approximately inversely proportional with the $CW_{min,i}$ value [10] for its DCF with the approximation improving with larger $CW_{min,i}$ choices which come at the expense of reducing the channel utilization parameter τ.

In [10], Contention Window Scaling Protocol (CWSP) is proposed to cope with the rate (performance) anomaly problem. In this model, the minimum contention window of each station is adjusted according to the ratio of the maximum data rate of the standard and the data rate of each station. Minimum Contention Window (CW_{min}) calculation for CWSP is given as follows,

$$\frac{CW_{min,i}}{CW_{min,base}} = \frac{R_{max}}{R_i} \tag{4.10}$$

In equation (4.10), $CW_{min,base}$ is the predefined CW_{min} parameter that is used as a baseline in the scaling operations and it is not specified in [10], R_{max} is the maximum data rate defined in the standard and R_i is the data rate of the station s_i. However, this model suffers from several drawbacks [33]. Consider an IEEE 802.11a DCF network where there are two stations A and B with data rates of 9

Mbps and 18 Mbps, respectively. According to IEEE 802.11a DCF standard, the minimum contention window size is 16, and the maximum data rate is 54 Mbps. When $CW_{min,base} = 16$ is used for CWSP, station A multiplies its minimum contention window size (16) by 6, and station B multiplies its minimum contention window size (16) by 3. Therefore station A and B uses 96 and 48 as CW_{min}, respectively. However, airtime fairness in this scenario can be simply satisfied by using 32 and 16 as CW_{min} for stations A and B, respectively. Therefore, the scaling of the contention window size should be based on the highest data rate among stations rather than the maximum possible data rate that is defined in the standard.

Scaling protocol that adjusts contention window size according to the highest data rate in the wireless LAN, is denoted as Optimal Scaling Protocol (OSP) in [33]. In the OSP model, it is assumed that the highest data rate, i.e. the fastest station's data rate, is announced by AP and known by all stations in the network. $CW_{min,i}$ calculation for the OSP model to achieve airtime fairness is given as follows,

$$\frac{CW_{min,i}}{CW_{min,base}} = \frac{R_f}{R_i} \tag{4.11}$$

where R_f is the data rate of the fastest station in the network and $CW_{min,base}$ is again the baseline minimum contention window size. Since the fastest station's data rate is announced by AP to all stations, the fastest station uses $CW_{min,base}$ as minimum contention window size and we will denote it as $CW_{min,f}$ for the OSP model. However, CWSP and OSP models suffer from another drawback [33]. In the IEEE 802.11 WLANs, we consider the use of a UDP/IP protocol stack and a layer 3 information packet that consists of the payload, the associated timestamps, and also the overhead introduced by the IP, UDP, and application layers. Further MAC and PHY encapsulation procedures are applied to the information packet before transmitting through the network. Information packets are transmitted by using the data rate of the station whereas some part of the PHY Header is transmitted via more robust Modulation and Coding schemes, which we refer it as the control rate in this study. For large packet sizes, data rate dominates the transmission time calculation and it can be directly used for

$CW_{min,i}$ scaling policy. However, as packet size decreases, transmission time deviates from $\frac{Packet\ size}{R_i}$ due to transmission of some parts of the PHY header with control rate. To have long-term equal airtime for all stations, transmission time for each station should be considered in scaling operations by taking into account packet sizes and protocol overheads. In our study, we assume that the average packet size is fixed throughout the network. We use the slightly improved model of OSP for the airtime access mechanism by using transmission times in scaling operations.

$$\frac{CW_{min,i}}{CW_{min,base}} = \frac{T_i}{T_f} \tag{4.12}$$

where T_i is the transmission time of source s_i and T_f is the transmission time of the fastest source in the network. Again, for an improved OSP model, the minimum contention window size of the fastest station, $CW_{min,f}$ is equivalent to the $CW_{min,base}$ as in the OSP model. In the numerical examples of the study, we set the $CW_{min,i}$ parameter of each station such that the p_i values equal to the expressions given as in equations (4.1), (4.3) and (4.9) for LCA, PFCA, and SPCA, respectively. Since each source uses the same CW_{min} parameter in LCA, all stations have equal long-term channel access probability, p_i. For practical implementation of the PFCA mechanism, the improved OSP scaling policy given in equation (4.12) is used. On the other hand, performance improvement for improved OSP compared to OSP and CWSP is demonstrated in Chapter 5 with simulation examples. For the proposed SPCA model, distributed airtime fair scaling policies can be directly modified and used. For the practical implementation of SPCA, the following scaling policy is used.

$$\frac{CW_{min,i}}{CW_{min,base}} = \sqrt{\frac{T_i}{T_f}} \tag{4.13}$$

Since there is a requirement for CW_{min} to be an integer, a rounding operation is applied after scaling and square root operations. In LCA, PFCA, and SPCA mechanisms, ratios between contention window sizes of peers are adjusted. However, the optimal choice for initial contention window size for the fastest source ($CW_{min,f}$) is still an open question. In [35], Bianchi et. al. proposed a mathematical model to find an optimal minimum contention window size for CSMA/CA

based WLANs. In this model, the optimal contention window size is calculated by a set of equations and these equations consider the transmission time of packets, number of stations in the network, and probability of collision. However, Bianchi's model is valid for single-rate networks when all stations have the same traffic load and $m = 0$, i.e. fixed backoff window size. Also, the model is mainly designed for networks with a low number of stations and may not be suitable for networks with a high number of stations. Therefore, using Bianchi's model to find an optimal $CW_{min,f}$ for this study is not feasible. This question is left for future work. In our simulation results, optimal $CW_{min,f}$ selection for each mechanism is selected in an offline manner. Details of $CW_{min,f}$ selection are given in Chapter 5.

4.5 Clarification of Scaling Policies

Three different scaling policies namely CWSP, OSP, and improved OSP, are explained for airtime fairness in Section 4. Although, we use equation (4.12) for the PFCA mechanism and equation (4.13) for the SPCA mechanism, it is possible to use equation (4.10) and (4.11) for PFCA mechanism and modified versions of these equations for SPCA mechanism, which are named as PFCA-CWSP, PFCA-OSP, SPCA-CWSP, and SPCA-OSP respectively. To visualize and clarify explained scaling policies, an example scenario is considered for a network with stations that have data rates of 6 Mbps, 18 Mbps, and 36 Mbps. $CW_{min,base}$ is taken as 16 for this example.

The possible highest data rate in the network is 54 Mbps according to the IEEE 802.11a DCF standard [1]. When CWSP is used for PFCA and SPCA mechanisms, the CW_{min} parameter of each station is adjusted based on the highest data rate in the standard, i.e. 54 Mbps. Resulting $CW_{min,i}$ selections for 3 different mechanisms are shown in Fig. 4.1 when CWSP is used. For LCA, each station uses a CW_{min} size of 16. This results in a *performance anomaly* problem. In PFCA-CWSP, performance anomaly is solved by scaling CW_{min} of each station according to the highest data rate in the standard which is 54 Mbps.

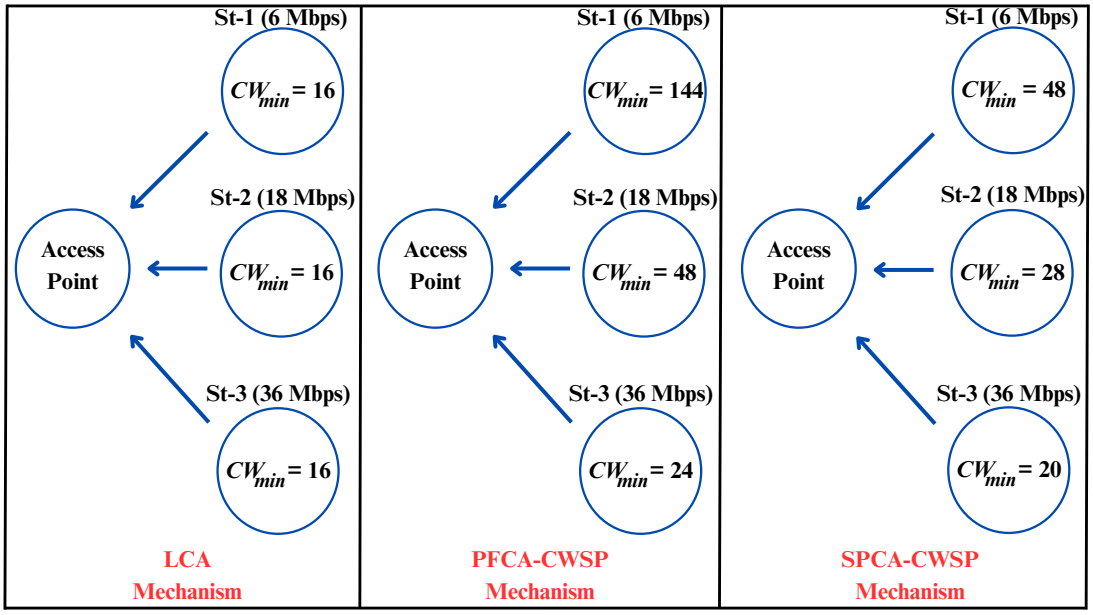

Figure 4.1: Scaling policies for LCA, PFCA, SPCA models when CWSP is used

In SPCA-CWSP, CW_{min} size of each station is adjusted as inversely proportional with the square root of the data rate of the station, with the goal of minimizing system PAoI. This scaling policy is far away from the optimal point because of two following reasons: Firstly, idle time in the network is increased because of unnecessary scaling operations based on the highest data rate defined in the standard which results in longer backoff processes and larger long-term idle duration. Secondly, CWSP loses its airtime fairness property with decreasing packet size. On the other hand, the CWSP policy is a completely distributed mechanism since it does not require any information from AP. To have a better model with less idle time, the OSP model can be used for the considered example scenario. The resulting $CW_{min,i}$ parameters for OSP policy are given in Fig. 4.2.

As it is shown in Fig. 4.2, the fastest station's data rate is used in scaling operations. Therefore, $CW_{min,f}$ is equal to the $CW_{min,base}$ in this model. Thanks to this model, idle time is reduced in the network. To get a more precise model, we have assumed that AP announces this information and all stations in the network are aware of the highest data rate in the network. However, OSP requires

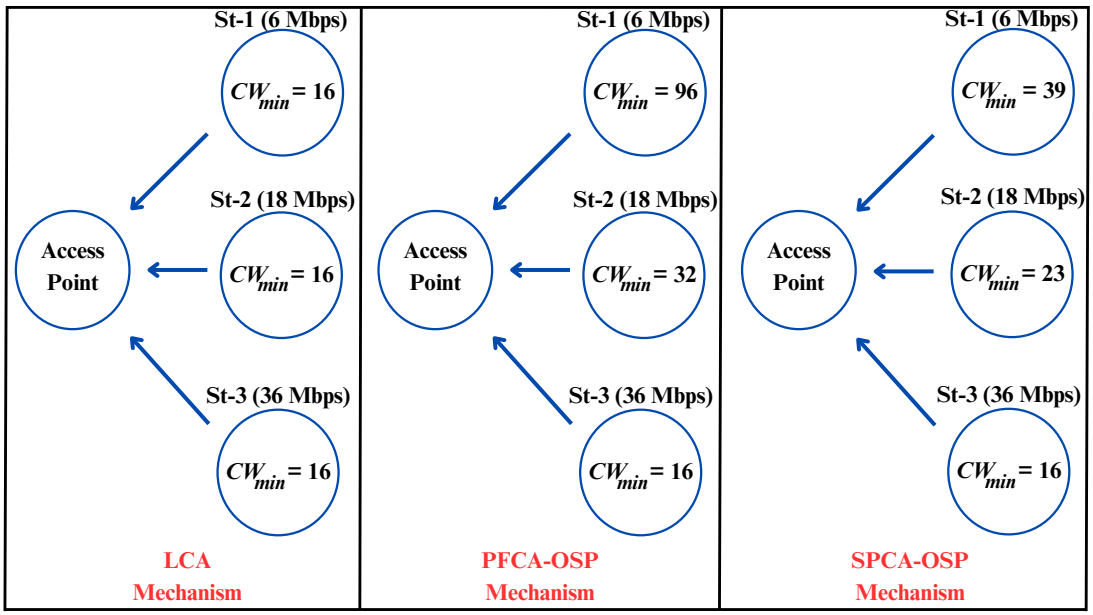

Figure 4.2: Scaling policies for LCA, PFCA, SPCA models when OSP is used

information on the highest data rate in the network which prevents OSP to be a completely distributed mechanism. The problem of this scaling policy is as follows. The transmission time of a packet deviates more from the division of packet size to the data rate as packet size decreases and using data rates for CW_{min} scaling operation results in unnecessarily larger CW_{min} parameters for stations with lower transmission rates. Therefore, instead of using data rates for scaling operations, transmission rates are used in the improved OSP model. For the considered scenario, resulting $CW_{min,i}$ parameters for improved OSP policy are given in Fig. 4.3.

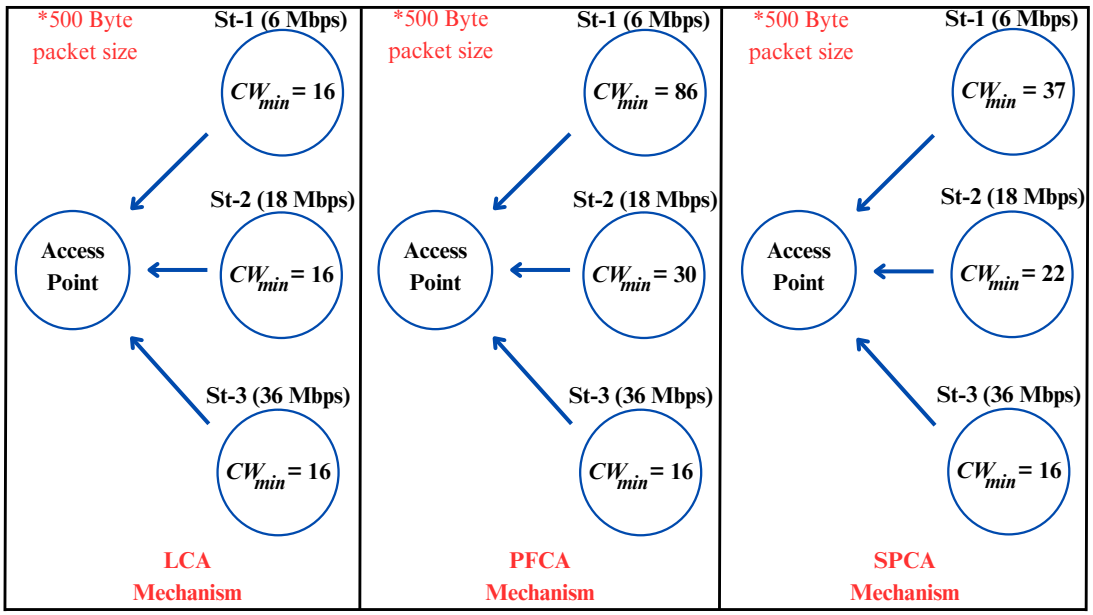

Figure 4.3: Scaling policies for LCA, PFCA, SPCA models when improved OSP is used

Transmission time for each station is calculated using the encapsulation process and timing features considered in [11]. Therefore, when 500 Byte packet size is used, scaling for $CW_{min,i}$ sizes of St-1, St-2, and St-3 should be by $(5.391, 2.862, 1)$, respectively, instead of $(6, 3, 1)$ for PFCA. The parameters that are used to calculate scaling weights are explained in Chapter 5. When SPCA is used, scaling of $CW_{min,i}$ sizes of St-1, St-2 and St-3 should be by $(2.322, 1.692, 1)$. Therefore, for PFCA and SPCA scenarios given in Fig. 4.3, we have used $(5.391, 2.862, 1)$ and $(2.322, 1.692, 1)$ instead of $(6, 3, 1)$ and $(\sqrt{6}, \sqrt{3}, 1)$ as scaling weights respectively for 500 Byte packet size.

Chapter 5

Numerical Results

We used a Python-based IEEE 802.11a DCF Simulator [11] to validate the model that is proposed in this study. The simulator in [11] has been validated by comparing the results gathered with analytical DCF models and ns-3, which is an open-source discrete-event network simulator and it is commonly used for research in the literature of computer networking [36]. A network with single-rate stations and LCA is considered in [11]. We modified the study in [11] to be able to compare different channel access mechanisms in a multi-rate IEEE 802.11a network. To simplify the simulation process, we assumed the propagation delay between contending stations and AP is negligible.

5.1 Encapsulation Process for Simulation Environment

In the IEEE 802.11 WLANs, we envision the use of a UDP/IP protocol stack and a layer-3 information packet consisting of the payload in the form of a status update packet and the associated timestamps, and also the overhead introduced by the IP, UDP, and application layers. The information packet is then encapsulated with MAC and PHY layer headers in which case it is called an information frame

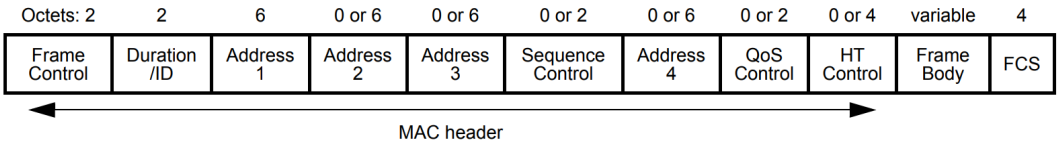

Figure 5.1: General MAC frame defined in the IEEE 802.11 standard [1]

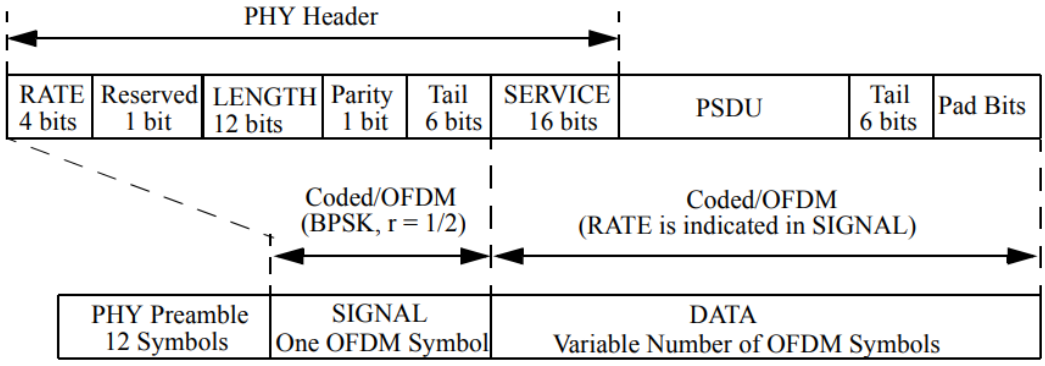

Figure 5.2: PPDU format defined in the IEEE 802.11 standard [1]

which is transmitted through the IEEE 802.11 wireless LAN network. We used the general MAC frame format which is defined in the IEEE 802.11 standard and it is shown in Fig. 5.1.

We have considered the maximum MAC header size in our simulations and we named the combination of MAC header and FCS fields that are shown in Fig. 5.1 as MAC Overhead (40B). The encapsulation process in the Python-based IEEE 802.11a DCF simulator [11] is as follows. An information packet, which includes payload and additional layer-3 information, is encapsulated at the MAC layer (MAC Overhead is appended) and MAC Protocol Data Unit (MPDU) is generated, which is equivalent to the Physical Layer Service Data Unit (PSDU). Service field (16b), Tail field (6b), and padding bits are added to the PSDU to generate MAC Common Part Sublayer Data Unit (CPSDU). CPSDU is shown as DATA in Fig. 5.2 and it is further encapsulated with necessary PHY header fields and PHY preamble to create a Physical Protocol Data Unit (PPDU) that is transmitted through the channel to the designated station. PPDU format defined in the standard is shown in Fig. 5.2.

The IEEE 802.11a DCF standard defines PHY preamble duration as 16 μs which is not dependent on the transmission rate of the station. Therefore, using data rate ratios for contention window scaling for small packet sizes moves the proposed mechanism away from the optimal point. Fixed preamble duration is one of the main reasons (using control rate for some parts of transmitted packet is another reason) that we decide to use transmission rate in contention window scaling operations instead of data rates.

5.2 Simulation Parameters and Considered Scenarios

We compared LCA, PFCA, and SPCA channel access mechanisms in terms of system peak AoI, system AoI, and throughput. As explained in Chapter 4, we propose a model that adjusts the minimum contention window size of each station according to the transmission rate of the station and the fastest station's transmission rate. Contention window scaling is applied to stations except stations with the highest transmission rate in the network. We denote the minimum contention window size of the fastest peer in the network as $CW_{min,f}$. There is still an open question which is the selection of $CW_{min,f}$ based on the configuration of the network. Also, as re-transmission occurs, the age of the received status update message will increase. At every re-transmission opportunity, the source s_i initiates a new sampling process to generate a fresh information packet, and the original status update packet is replaced with the fresh packet. Keeping and transmitting the original information packet generated at the first transmission opportunity for energy efficiency purposes is left outside the scope of this study. Table 5.1 shows the parameters of the CSMA/CA based IEEE 802.11a DCF Simulator used in the simulations for performance evaluation.

IEEE 802.11a DCF standard defines the DIFS, SIFS, slot duration, MAC overhead, re-transmission limit, and PHY preamble duration as listed in Table I. We assume that all contending stations use 20 MHz bandwidth for the transmission

Table 5.1: IEEE 802.11a DCF based simulation parameters

Parameters	Value
DIFS	34 μs
SIFS	16 μs
Slot Duration	9 μs
PHY Preamble Duration	16 μs
ACK Timeout	45 μs
MAC Overhead	40 Bytes
Additional Overhead	22 bits + Padding bits
Data Rates	6,9,12,18,24,36,48,54 Mbps
Control Rates	6,6,12,12,24,24,24,24 Mbps
Retransmission limit	7

and for 20 MHz channel spacing, there are eight possible data rates for a station, which are listed in Table 5.1 and supporting data rates of 6, 12 and 24 Mbps are mandatory for each station. According to IEEE 802.11 standard [1], the SIGNAL field in PPDU, as shown in Fig. 5.2, and ACK messages should be transmitted by using BPSK and 1/2 code rate. Although the standard suggests using the most robust Modulation and Coding Scheme (MCS) to transmit SIGNAL field and ACK messages, which results in a 6 Mbps control rate (transmission rate for the SIGNAL field and ACK), the data rate-control rate pairs are selected as listed in Table 5.1 for the simulator in [11]. As shown in Table 5.1, the control rate for each MCS is selected from the three mandatory data rates in a way that the selected control rate is the maximum mandatory rate that is smaller than or equal to the corresponding data rate. There are 8 Modulation and Coding Schemes (MCS) defined in the simulator and each MCS has a specific data rate and control rate. Each MCS is named from MCS-0 to MCS-7. Data rate-control rate pair for each MCS defined in the simulator [11] are shown in Table 5.2. Modulation types and coding rates in Table 5.2 are given for data rates.

As shown in Table 5.2, 8 MCS types are defined in the IEEE 802.11a DCF standard. Since we assume stationary stations throughout the network for the simulations, we assigned a fixed MCS for each station. The assignment process is applied by considering two models whose distributions are shown in Fig. 5.3.

Random variables shown in Fig. 5.3, indicate modulation and coding scheme

Table 5.2: MCS parameters for IEEE 802.11a DCF WLANs (except control rates)

	Modulation	Coding rate	Resulting Data Rate (Mbps)	Used Control Rate (Mbps)
MCS-0	BPSK	1/2	6	6
MCS-1	BPSK	3/4	9	6
MCS-2	QPSK	1/2	12	12
MCS-3	QPSK	3/4	18	12
MCS-4	16 QAM	1/2	24	24
MCS-5	16 QAM	3/4	36	24
MCS-6	64 QAM	2/3	48	24
MCS-7	64 QAM	3/4	54	24

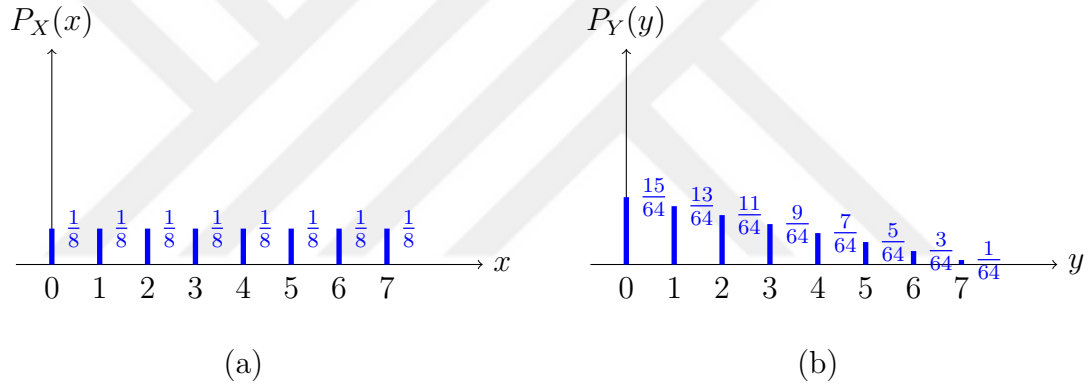

Figure 5.3: PMFs for uniformly (a) and circularly (b) distributed cases

labels that are shown in Table 5.2. In Fig. 5.3-a, $P_X(x)$ is presented which represents a uniformly distributed mixture scenario, where each MCS has the same probability of being assigned to the station. For $P_Y(y)$ function, we have considered a scenario where stations are placed in a circular area. For this scenario, we have assigned MCS to the stations according to distance from AP (located at the center), which is the absolute distance to the center of the circular area. The circular mixture model can be envisioned as concentric nested circles where the AP is located at the center of the circle and then the data rate of the station is selected based on its distance from the AP. A basic representation of the circular scenario is shown in Fig. 5.4.

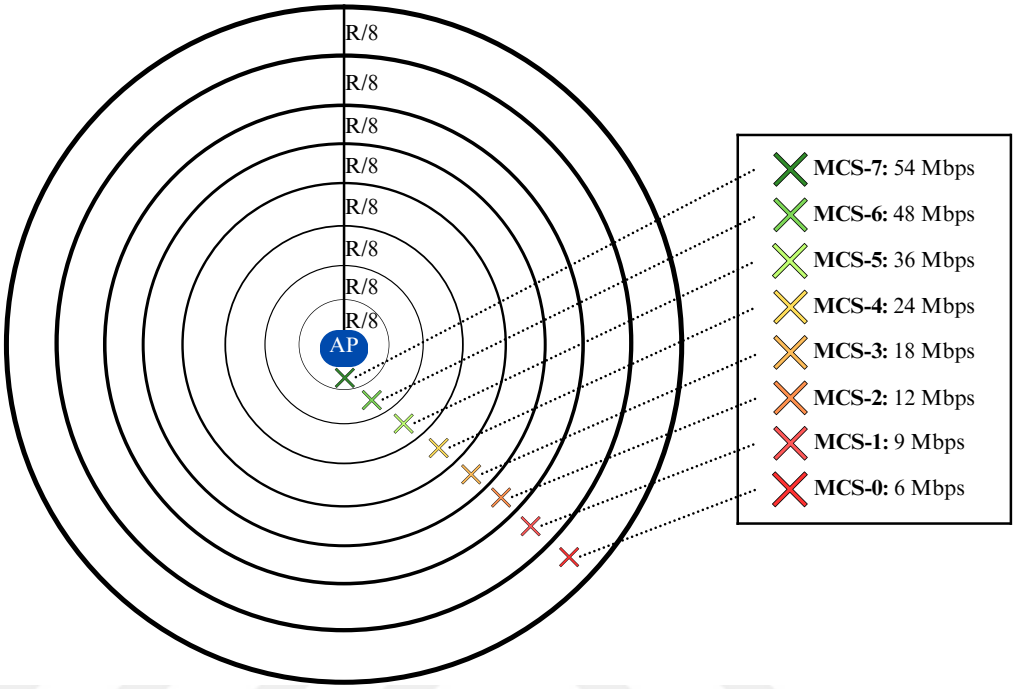

Figure 5.4: Representation for circularly distributed case

5.3 Performance Comparison of CWSP, OSP, and Improved OSP Models

Before moving on to the comparison of LCA, SPCA, and PFCA mechanisms, at first, we validate the performance improvement for improved OSP scaling policy by simulation. As explained previously, $CW_{min,i}$ scaling policy for PFCA can be based on equation (4.10), (4.11), or (4.12). It is known that airtime fairness between stations increases if we use equation (4.12) for scaling instead of others. We measured the airtime usage of each station when CWSP, OSP, and improved OSP mechanisms are used to observe performance improvement in terms of airtime fairness. Also, it is known that increasing $CW_{min,base}$ results in an improvement in providing airtime fair model [8]. Simulation parameters for airtime fairness comparison are provided in Table 5.3.

As explained in Section 4.4, $CW_{min,base}$ parameter is equivalent to the $CW_{min,f}$

Table 5.3: Simulation parameters for airtime fairness

Parameter	Value
Packet Size	300 B
Number of Stations	7
MCS list	(0,1,2,3,4,5,6)
Methods	PFCA-CWSP, PFCA-OSP, PFCA
$CW_{min,base}$	64
CW_{max}	1024

for OSP and improved OSP models. We considered a network with 7 stations (from s_1 to s_7) in which the fastest station has a data rate of 48 Mbps (MCS values are shown in Table 5.3 for each station respectively). We compared three mechanisms listed in Table 5.3 in which PFCA indicates the mechanism with scaling based on transmission times, i.e., improved OSP. By using the simulation parameters given in Table 5.3, we observed the difference between CWSP, OSP, and improved OSP mechanisms. Results for the PFCA mechanism based on CWSP, OSP, and improved OSP are provided in Table 5.4.

Table 5.4: Channel utilizations for each station when PFCA-CWSP, PFCA-OSP, PFCA (Improved OSP) mechanisms are used

	s_1	s_2	s_3	s_4	s_5	s_6	s_7
τ_i (CWSP)	0.056	0.058	0.060	0.063	0.065	0.069	0.074
τ_i (OSP)	0.058	0.059	0.060	0.065	0.067	0.072	0.077
τ_i (Improved OSP)	0.067	0.066	0.066	0.069	0.069	0.070	0.070

As seen in Table 5.4, air-time usage of stations with different data rates gets closer to each other as improved OSP mechanism is used. If we increase $CW_{min,base}$ parameter further, we will achieve closer airtime usages between sources. Also, it is observed that total channel utilization, τ of PFCA-CWSP, PFCA-OSP, and PFCA are 0.445, 0.458, and 0.477, respectively. Since CWSP unnecessarily scales CW_{min} of stations based on the highest data rate defined in the standard, increased idle time results in lower channel utilization. Also, the PFCA-OSP mechanism uses data rates for scaling operations which deviates from the transmission ratio as packet size decreases. Due to larger scaling, idle time again increases which results in lower channel utilization compared to PFCA (improved OSP) mechanism. Therefore, we used improved OSP, i.e., equation (4.12) for the PFCA mechanism in our simulations. As we know that increasing air-time

fairness leads to a higher sum of logarithms of throughputs, we compared PFCA-CWSP, PFCA-OSP, and PFCA mechanisms in terms of the sum of logarithms of throughputs. Simulation parameters in Table 5.5 are used.

Table 5.5: Simulation parameters for the comparison of CWSP, OSP, and improved OSP models (PFCA)

Parameter	Value
Packet Size	300 B
Simulation time	300 s
Number of Stations	12
MCS list	(0,1,2,3,4,5,6)
Methods	PFCA-CWSP, PFCA-OSP, PFCA
$CW_{min,base}$ alternatives	16,32,64,128,256
CW_{max}	4096

The simulation results are shown in Fig. 5.5.

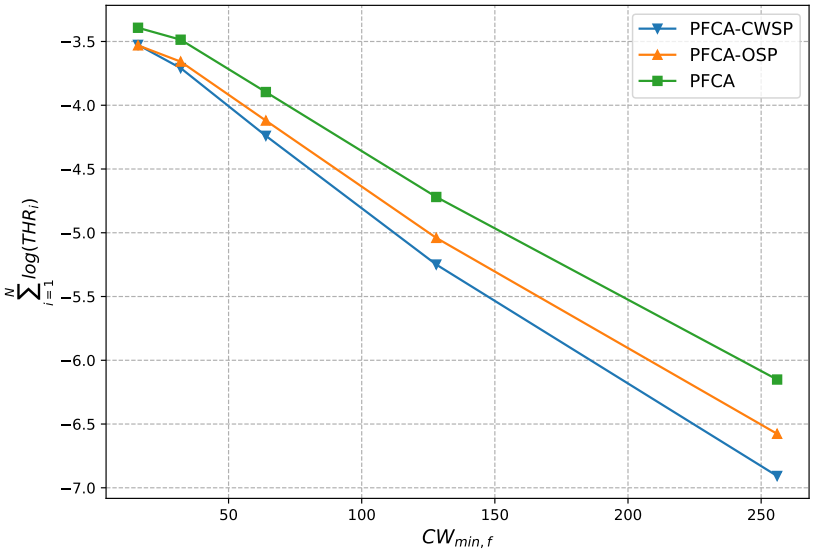

Figure 5.5: Simulation results for comparison of PFCA-CWSP, PFCA-OSP, and (Improved OSP) PFCA

As seen in Fig. 5.5, PFCA mechanism results in higher $\sum_{i=1}^{N} log(THR_i)$ for different $CW_{min,f}$ parameters where THR_i denotes the throughput of source s_i.

This occurs since PFCA results in a more accurate airtime fair model. To observe the performance improvement in system PAoI results for SPCA compared to SPCA-CWSP and SPCA-OSP mechanisms, we have considered the simulation parameters given in Table 5.5 without access mechanisms. As the success of the airtime fair model increases, the proposed model with the goal of minimizing system PAoI becomes more successful. We compared three mechanisms namely, SPCA-CWSP, SPCA-OSP, and SPCA (improved OSP) in terms of system PAoI to observe the performance improvement which directly depends on the success of the air-time fair model. The simulation results for this simulation are shown in Fig. 5.6.

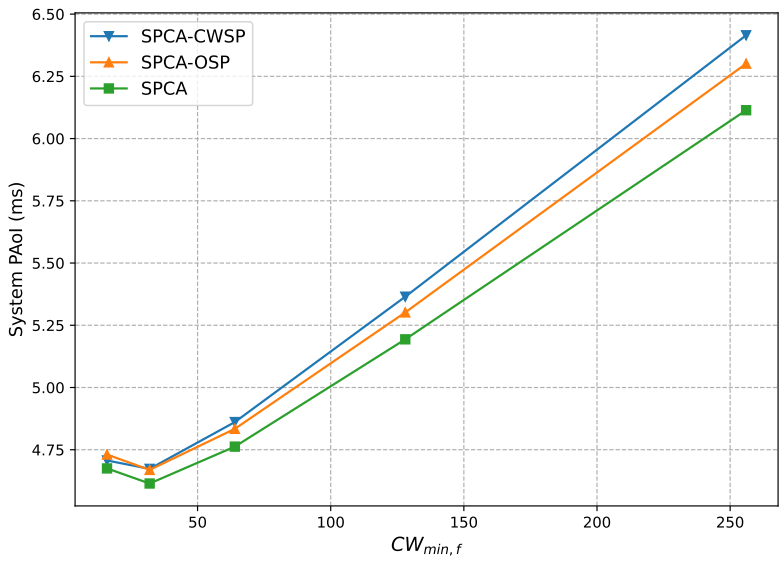

Figure 5.6: Simulation results for comparison of SPCA-CWSP, SPCA-OSP, and (Improved OSP) SPCA

We considered a set of $CW_{min,f}$ parameters to compare three mechanisms fairly. As shown in Fig. 5.6, the system PAoI of SPCA is smaller than SPCA-OSP and SPCA-OSP has a smaller system PAoI than SPCA-CWSP for the same $CW_{min,f}$ selections that are given in Table 5.5. $CW_{min,f}$ is the data rate of the fastest station for SPCA-OSP and SPCA mechanisms but in SPCA-CWSP, the fastest station scales its CW_{min} since the scaling operation is applied according

to the fastest data rate defined in the standard which is larger than the data rate of the fastest station in the network. The result is expected since improved OSP provides a more accurate airtime fair model when it is used for the PFCA mechanism. Therefore, when we directly used improved OSP for the SPCA mechanism by applying simple square root operation, we end up with more lower system PAoI compared to CWSP and OSP mechanisms. According to the simulation results that are shown in Figs. 5.5 and 5.6, we validated using an improved OSP model, which uses transmission times for scaling operations, for PFCA and SPCA mechanisms.

5.4 Moving Average Age Statistics for Sample Configuration

First, we considered the most straightforward scenario for simulation. In this scenario, there is one station from each data rate that is defined in the IEEE 802.11a DCF standard in the network. Simulation parameters for the first scenario are given in Table 5.6.

Table 5.6: Simulation parameters for the comparison of CA mechanisms

Parameters	Value
Packet Size	500 B
Number of stations	8
$CW_{min,f}$	16
Simulation Duration	300 s
Methods	LCA, PFCA, SPCA
Retransmission limit	7
CW_{max}	1024

The average PAoI and AoI statistics of each station are measured at Access Point. In Table 5.6, 300-sec simulation duration might be considered short but there are over 699,000 successful packet transmissions for each channel access mechanism during the simulation time. Simple Moving Average (SMA) technique is used to understand the underlying patterns over time for each channel access

mechanism. The resulting moving average PAoI plots for LCA, PFCA, and SPCA are shown in Fig. 5.7.

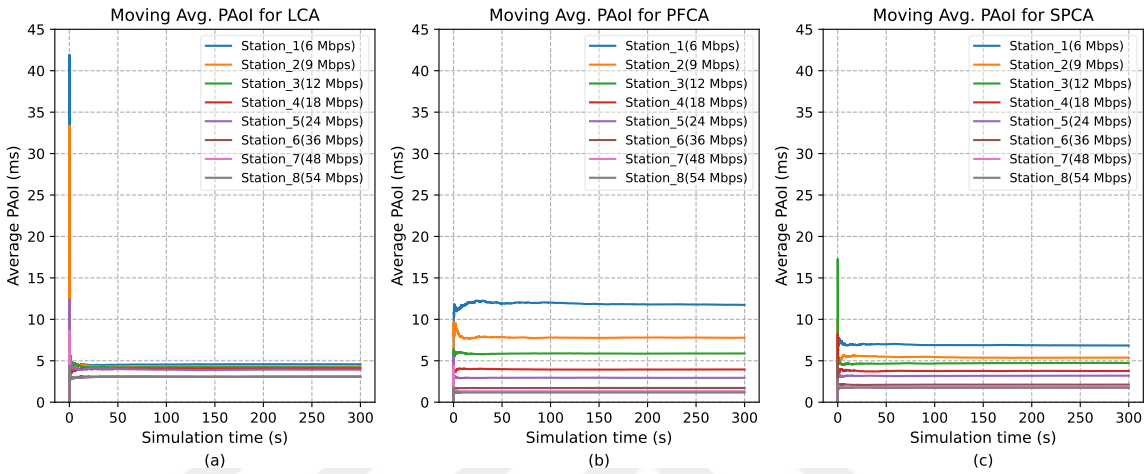

Figure 5.7: Moving Average PAoI results for LCA, PFCA, and SPCA

As shown in Fig. 5.7, the average PAoI of each station for LCA is nearly the same for stations with different data rates, which results from equal channel access probability between stations. As it can be seen from Fig. 5.7-a, stations with lower data rates have slightly higher average PAoI than higher data-rated stations. This occurs because of the following feature. When a status update message is received by AP, age drops to the transmitter's transmission time T_i (see Fig. 3.1) instantly. Therefore, stations with higher data rates have slightly less average PAoI for the LCA mechanism. Since the channel access probability of each station is the same in LCA, the average PAoI results for different stations are close to each other. When PFCA is used, channel access probabilities of fast stations are increased compared to slow stations. Therefore, average PAoI results of high data-rated stations are improved compared to LCA. On the other hand, channel access probabilities of stations with low data rates are decreased. Hence slow stations can not transmit their status update messages for a longer time compared to fast stations and this results in an abrupt increment in average PAoI for slow stations, which leads to a greater average peak age difference between different rated stations. In SPCA, average PAoI differences between stations are decreased compared to PFCA but gaps are still larger compared to LCA as can be seen in Fig. 5.7. This happens as we scale CW_{min} of each station as proportional

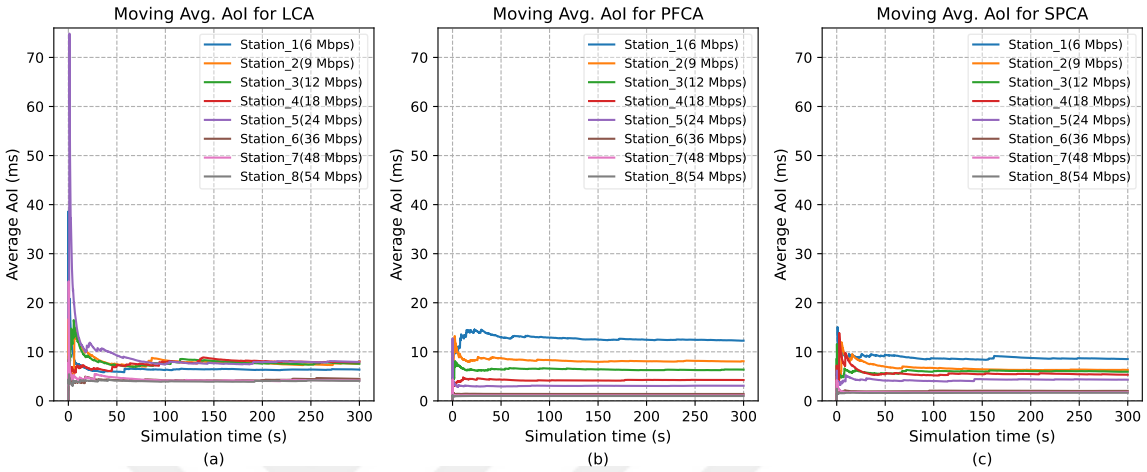

Figure 5.8: Moving Average AoI results for LCA, PFCA, and SPCA

to the square root of the transmission time. As explained in Chapter 4, for PFCA, stations with low transmission rates scale their CW_{min}, which results in a decrease in channel access probability. Therefore stations with low transmission rates can not transmit their status update packets for a long time, which results in increase for age statistics. On the other hand, in LCA, when stations with low transmission rates get the channel, they occupy the channel for a long time, which results in increase in the overall age statistics of stations with high transmission rates. SPCA provides a balance between these two channel access mechanisms. Although our proposed model is designed to reduce system PAoI, we measured the performance of the proposed model in terms of AoI. Moving average AoI results for LCA, PFCA, and SPCA are shown in Fig. 5.8.

Similar responses and patterns are observed in Fig. 5.8 for Moving Average AoI plots. However, there is a critical difference in AoI plots. There are more jumps and more instability in average AoI plots. This instability results from the average AoI being more sensitive to collisions. When a station can not transmit its status update message to Access Point for a long time, the average AoI pattern is greatly affected by the starvation of successfully transmitting the status update packet. System PAoI and AoI results are given in Table 5.7.

As given in Table 5.7, channel utilization for LCA is higher than other channel

Table 5.7: Simulation results for Moving Average age statistics

Parameters	**LCA**	**PFCA**	**SPCA**
System PAoI (ms)	3.785	4.563	3.703
System AoI (ms)	6.340	4.698	4.485
Channel Utilization	0.664	0.616	0.643
Throughput (Mbps)	9.324	13.748	11.623
Collision Probability	0.1738	0.0768	0.117

access mechanisms for the example scenario. This occurs as stations with low data rates occupy the channel for a long time when they access the channel in the LCA mechanism, which results in less idle time due to less frequent protocol signaling and packet transmission (duration due to ACK messaging and idle time due to backoff process reduces). Therefore LCA results in higher channel utilization. Higher channel utilization provides LCA an advantage in terms of age metrics. On the other hand, even though LCA has higher channel utilization than the proposed mechanism, SPCA is still a better mechanism to minimize system peak AoI.

Also, the performance anomaly problem for the LCA mechanism can be observed from Table 5.7. Performance anomaly is solved by using PFCA and the throughput of the system is increased. As it is expected, the proposed mechanism provides less channel access probability to stations with high data rates compared to PFCA which results in less channel throughput than PFCA. On the other hand, it can be observed that SPCA still provides higher throughput than LCA.

5.5 Effect of $CW_{min,f}$ on Age Metrics

As it is mentioned in Chapter 4, an online mechanism is required for $CW_{min,f}$ parameter selection. How to select the $CW_{min,f}$ parameter is not known in advance right now. $CW_{min,f}$ is a critical metric that directly affects channel utilization. We simulate a set of $CW_{min,f}$, and evaluate system age statistics for each $CW_{min,f}$ value to observe the effect of $CW_{min,f}$ on system PAoI and AoI. For this purpose,

we considered a scenario with settings given in Table 5.8.

Table 5.8: Simulation parameters for $CW_{min,f}$ effect ($N = 64$)

Parameters	**Value**
Packet Size	500 B
Station Number	64
Mixture Model	Uniform
$CW_{min,f}$ alternatives	$(16, 32, 64, 128, 256, 512, 1024, 2048)$
Simulation Duration	120 s
Methods	LCA, PFCA, SPCA
Retransmission limit	7
CW_{max}	16384

We consider a multi-rate network with a large number of stations (64) where the packet size is 500 Bytes to investigate the impact of the choice of the parameter $CW_{min,f}$ on system PAoI for LCA, PFCA, and SPCA. We assume a uniform mixture model where there is an equal number of stations for each standard data rate, i.e., 8 stations for each data rate given in Table 5.8. The simulations are conducted for different $CW_{min,f}$ parameters from the given $CW_{min,f}$ alternatives in Table 5.8. CW_{max} is set to 16384 for this simulation while CW_{max} is specified as 1024 in the IEEE 802.11a DCF standard. As CW_{min} of each station is adjusted in SPCA and PFCA except for the fastest station by using a scaling operation, CW_{max} is set to 16384 to guarantee that $CW_{min,i}$ does not exceed CW_{max} after the scaling. The simulation result for this simulation is shown in Fig. 5.9.

As shown in Fig. 5.9, $CW_{min,f}$ parameter has a significant effect on system PAoI and AoI. According to Fig. 5.9-a, LCA, PFCA, and SPCA do not follow the same pattern as $CW_{min,f}$ increases. At first, the system PAoI decreases up to a certain point as $CW_{min,f}$ increases because of the decrease in the probability of collisions. However, increasing $CW_{min,f}$ further causes larger idle times in the network which results in higher system PAoI and lower channel utilization. Therefore, there is a certain value for $CW_{min,f}$ which minimizes the system PAoI for the given channel access mechanism and this value appears to be different for each channel access mechanism of interest. Therefore comparing three mechanisms in terms of peak age statistics for a fixed $CW_{min,f}$ parameter might end up in incorrect inferences. We also observed that SPCA results in the lowest system

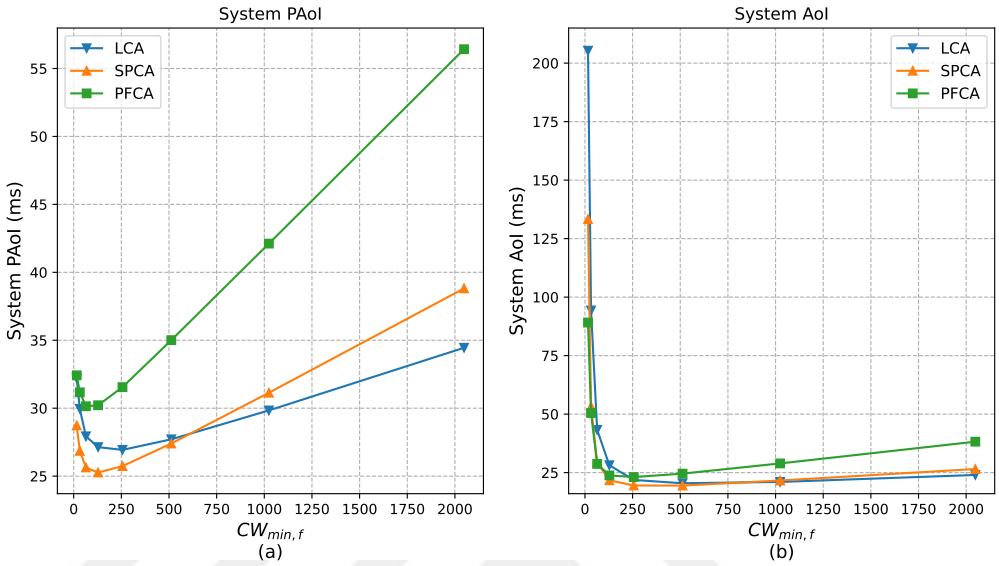

Figure 5.9: $CW_{min,f}$ effect on system PAoI and AoI for $N = 64$

PAoI among all the studied channel access mechanisms. We ordered the top 10 configurations with the minimum system PAoI results which is shown in Table 5.9.

Table 5.9: Detailed simulation results for $CW_{min,f}$ effect ($N = 64$)

Rank	Method	$CW_{min,f}$	Sys. PAoI (ms)	Sys. AoI (ms)	τ	P_{coll}	Throughput (Mbps)
1	SPCA	128	25.267	21.716	0.700	0.069	11.581
2	SPCA	64	25.640	29.306	0.686	0.124	11.404
3	SPCA	256	25.738	19.497	0.677	0.037	11.347
4	SPCA	32	26.858	53.271	0.647	0.204	10.848
5	LCA	256	26.932	21.861	0.732	0.054	9.613
6	LCA	128	27.135	28.149	0.726	0.099	9.541
7	SPCA	512	27.398	19.461	0.636	0.019	10.648
8	LCA	512	27.710	20.454	0.709	0.030	9.340
9	LCA	64	27.930	43.270	0.701	0.163	9.269
10	SPCA	16	28.733	133.304	0.613	0.287	10.295

As shown in Table 5.9, SPCA has the minimum system PAoI result among all possibilities with the correct $CW_{min,f}$ selection which is 128 in this scenario. If we compare the best results for SPCA (rank 1) and LCA (rank 5), we can state that although SPCA results in lower τ than LCA, it can still outperform LCA

mechanism in terms of system PAoI. One might think that a lower probability of collision always results in higher overall utilization but this is not the case. For example, configuration at 6^{th} ranking has a higher probability of collision than 1^{st} ranking but it also has higher overall utilization. This occurs because of equal channel access probabilities in LCA which leads to lower successful packet transmissions but more occupied channel. Another important observation is that even though system AoI and system PAoI are positively correlated, an increase in system PAoI does not necessarily lead to an increase in system AoI. When the probability of collision drastically increases, system AoI significantly gets affected. Also, as can be seen from Fig. 5.9-b, at first, the system AoI drastically decreases up to a certain point as $CW_{min,f}$ increases because of the decrease in the probability of collisions. On the other hand, increasing $CW_{min,f}$ further causes larger idle times in the network which results in higher system AoI and lower channel utilization. Since only the top 10 configurations are listed in Table 5.9, the PFCA mechanism can not be observed. Another scenario is considered with more stations to observe the effect of configuration on the $CW_{min,f}$ that minimizes system PAoI. All the parameters except the number of stations were kept the same. Simulation parameters are shown in Table 5.10.

Table 5.10: Simulation parameters for $CW_{min,f}$ effect ($N = 128$)

Parameters	**Value**
Packet Size	500 B
Station Number	128
Mixture	Uniform
$CW_{min,f}$ list	$(16, 32, 64, 128, 256, 512, 1024, 2048)$
Simulation Duration	120 s
Methods	LCA, PFCA, SPCA
Retransmission limit	7
CW_{max}	16384

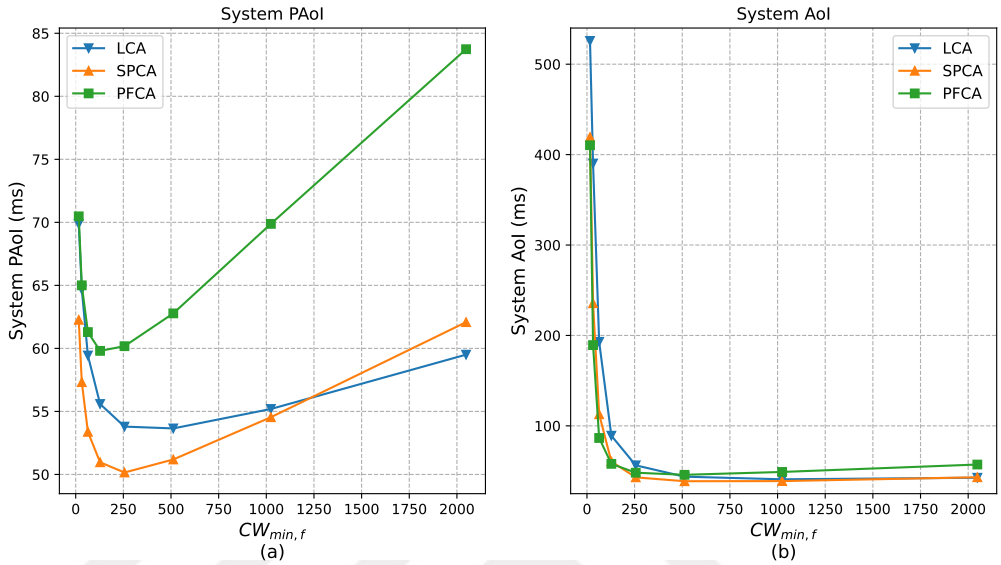

Figure 5.10: $CW_{min,f}$ effect on system PAoI and AoI for $N = 128$

Table 5.11: Detailed simulation results for $CW_{min,f}$ effect ($N = 128$)

Rank	Method	$CW_{min,f}$	Sys. PAoI (ms)	Sys. AoI (ms)	τ	P_{coll}	Throughput (Mbps)
1	SPCA	256	50.154	43.045	0.679	0.069	11.563
2	SPCA	128	50.964	60.545	0.669	0.124	11.399
3	SPCA	512	51.187	38.761	0.667	0.038	11.337
4	SPCA	64	53.380	112.850	0.645	0.203	10.861
5	LCA	512	53.652	43.799	0.741	0.055	9.595
6	LCA	256	53.796	56.343	0.739	0.098	9.572
7	SPCA	1024	54.541	38.911	0.641	0.0205	10.633
8	LCA	1024	55.193	40.885	0.723	0.031	9.325
9	LCA	128	55.588	89.140	0.709	0.164	9.267
10	SPCA	32	57.322	235.599	0.604	0.294	10.141

Simulation results for $N = 128$ are shown in Fig. 5.10 and Table 5.11. As it is shown in Fig. 5.9 and Fig. 5.10, system PAoI minimizing $CW_{min,f}$ value changes as configuration changes. Also, system AoI significantly gets affected by high collision and low channel utilization as shown in Fig. 5.9 and Fig. 5.10.

As shown in Table 5.11, compared to $N = 64$ scenario, higher $CW_{min,f}$ selections are necessary to have less system PAoI. Therefore, we decided to compare different mechanisms by using the optimal $CW_{min,f}$ selection that produces the minimum system peak age for each mechanism, i.e., optimum $CW_{min,f}$ selections in terms of system PAoI. In the following simulation results, LCA, SPCA, and PFCA mechanisms are compared by using the optimum $CW_{min,f}$ selection for each mechanism.

5.6 Performance Comparison of LCA, PFCA, and SPCA for Different Configurations

First, performances are compared for different packet sizes and networks with different numbers of stations. As explained previously, optimal $CW_{min,f}$ selection has a significant effect on channel utilization of the system. To compare three mechanisms fairly, $CW_{min,f}$ should be selected appropriately. Configuration dependent online $CW_{min,f}$ selection policy is necessary to further minimize system PAoI. Since we do not have an online mechanism for $CW_{min,f}$, the three channel access mechanisms LCA, SPCA, and PFCA are compared in the next simulation example by using a particular value of $CW_{min,f} \in \{16, 32, 64, 128, 256, 512\}$ that is obtained offline through simulations that minimizes the system PAoI. CW_{max} is set to 4096 for the following simulations to make sure that the CW_{min} parameter does not exceed CW_{max} after the scaling operation. Therefore, we evaluated each method for a list of $CW_{min,f}$ and compared the performance of each mechanism when the optimal $CW_{min,f}$ size, which results in minimum system PAoI among other values in the list, is selected. We showed that SPCA always results in better system PAoI than other existing mechanisms.

As shown in Table 5.1, we have considered two different mixtures to validate our model. In the first mixture, which is uniform, we have selected the data rate of each station uniformly from given set of data rates in Table 5.1, i.e., there is equal probability for the data rate of each station in the network. PMF of

uniform distribution is shown in Fig. 5.3-a. We have a fixed data rate for each station according to the distribution and calculate the age statistics for that fixed configuration instead of using Monte Carlo simulations. For the first scenario, we considered networks with 3 different packet sizes and 3 different numbers of stations when data rates are assigned according to the uniform mixture model. For example for the network with 64 (128) stations, there are 8 (16) stations for each data rate in the network. Considered simulation parameters for this scenario are given in Table 5.12.

Table 5.12: Simulation parameters for 9 different configurations when uniform mixture model is used

Parameters	**Value**
Packet Size	300,500,700 B
Station Number	64,128,192
Mixture	Uniform
$CW_{min,f}$ list	$(16, 32, 64, 128, 256, 512)$
Simulation Duration	120 s
Methods	LCA, PFCA, SPCA
Retransmission limit	7
CW_{max}	4096

We evaluated LCA, SPCA, and PFCA mechanisms for any combination of three different packet sizes and three different numbers of stations as provided in Table 5.12. The system PAoI, system AoI and channel throughput results for the uniform mixture model are shown in Fig. 5.11. As shown in Fig. 5.11-a, SPCA outperforms other schemes in terms of system PAoI for all 9 different simulation environments.

Fig. 5.11-a reveals that SPCA outperforms the other schemes in terms of system PAoI for all the studied network configurations. In particular, SPCA yields an improvement in system PAoI ranging from 4.31% to 7.93%, depending on the packet size and the number of stations N, compared to LCA, whereas the improvement ranges from 15.08% to 16.13% when the comparison is against PFCA. Although SPCA is devised to reduce the system PAoI, the performance is also evaluated in terms of the system AoI which is depicted in Fig. 5.11-b which shows that SPCA results in lower system AoI compared with the other two mechanisms

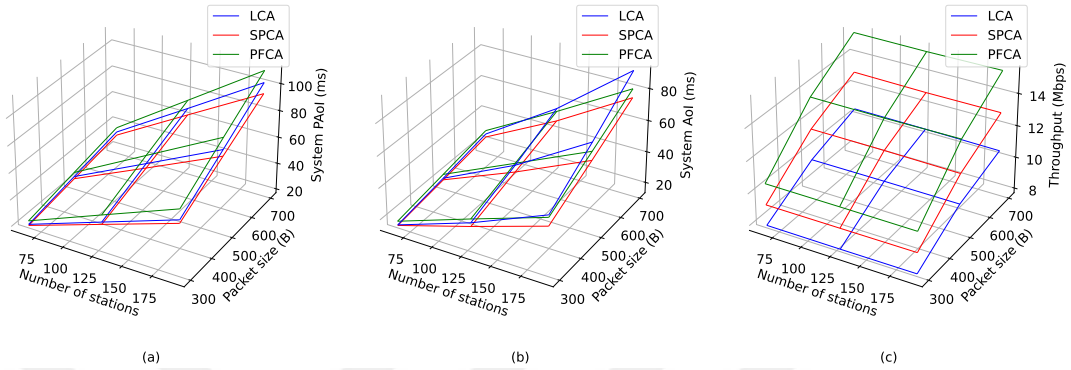

Figure 5.11: System PAoI (a), system AoI (b) and channel throughput (c) results for LCA, PFCA, SPCA when station's data rates are adjusted according to uniform mixture model.

for all the studied scenarios. Although enhancements in the system AoI are observed for the considered cases, SPCA does not guarantee improvement in the system AoI performance. To observe the trade-off between the throughput and system PAoI, we evaluated the total throughput for the studied access mechanisms as well. As shown in 5.11-c, PFCA outperforms the other mechanisms in terms of overall throughput. Although the performance reduction in terms of total throughput for SPCA compared to PFCA ranges from 12.39% to 16.63%, SPCA still provides better performance than LCA in terms of total throughput with the improvement ranging from 16.59% to 22.67%.

We repeated the same experiment in a circular mixture model where the stations are uniformly located within the circular coverage region. The circular mixture model can be envisioned as concentric nested circles where the AP is located at the center of the circle and then the data rate of the station is selected based on its distance from the AP. Therefore, the number of stations for each data rate (given in Table 5.1) is proportional to $\{15, 13, 11, 9, 7, 5, 3, 1\}$, respectively. The simulation parameters, given in Table 5.12, are used except for the mixture model. The simulation results for the circular mixture are given in Fig. 5.12.

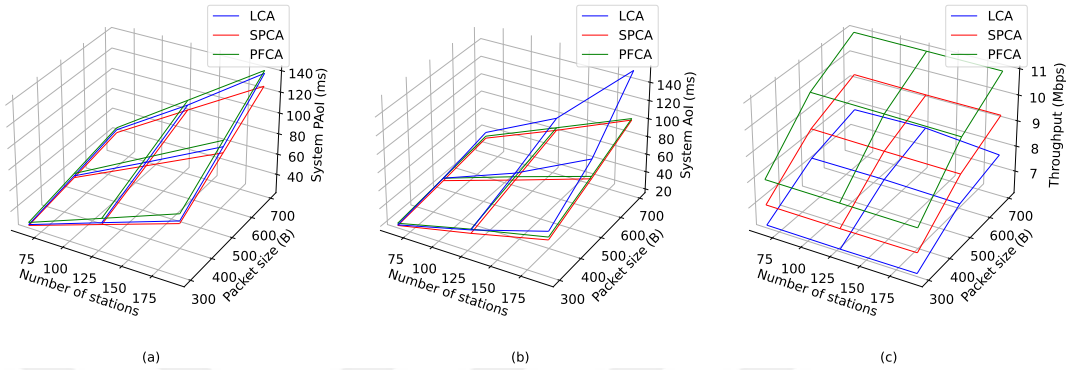

Figure 5.12: System PAoI (a), system AoI (b) and channel throughput (c) results for LCA, PFCA, SPCA when station's data rates are adjusted according to circular mixture model

We observed for the circular model that SPCA improves the system PAoI by 3.32% to 8.63% compared to LCA, and by 10.04% to 11.24% compared to PFCA. PAoI improvements appear to be smaller in the circular model compared with the uniform model since there are more stations with lower data rates in the circular model.

Lastly, we considered a network in which only MCS-0 (lowest data rate) and MCS-7 (highest data rate) are used. We measured the performance of the mechanisms for different Low Station Ratio (LSR) parameters. Simulation parameters for LSR simulation are shown in Table 5.13.

Table 5.13: Simulation parameters for 9 different configurations to observe LSR effect

Parameters	**Value**
Packet Size	300,500,700 B
Station Number	50
LSR Parameters	0.2, 0.5, 0.8
$CW_{min,f}$ list	$(16, 32, 64, 128, 256, 512)$
Simulation Duration	120 s
Methods	LCA, PFCA, SPCA
Retransmission limit	7
CW_{max}	4096

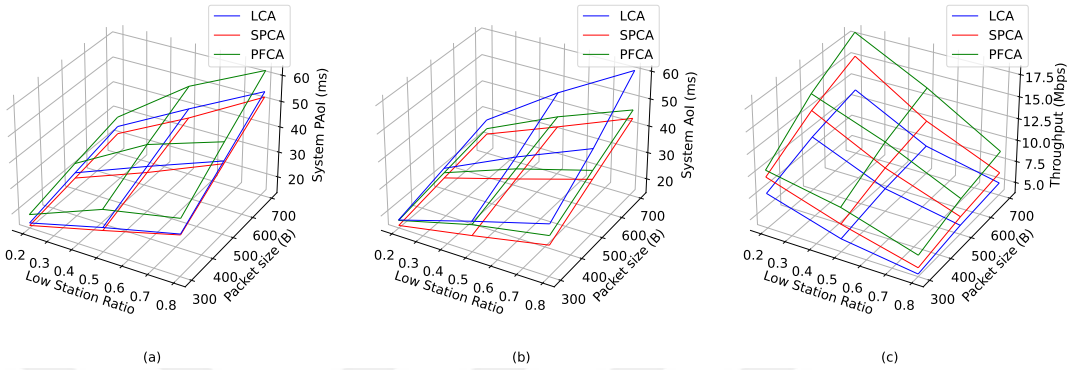

Figure 5.13: System PAoI (a), system AoI (b) and channel throughput (c) results for LCA, PFCA, SPCA when station's data rates are adjusted according to different LSR parameters

Simulation results for system PAoI, system AoI, and throughput are shown in Fig. 5.13. As shown in Fig. 5.13, SPCA results in better system AoI and system PAoI performances compared to LCA and PFCA mechanisms for the considered scenario. Additionally, system PAoI result differences for a fixed number of stations and packet size for different mechanisms are more significant for the $LSR = 0.5$ case. Therefore SPCA provides greater performance in terms of system PAoI when there is an equal number of stations from two classes for the considered simulation. Particularly, SPCA provides an improvement in system PAoI ranging from 1.13% to 12.04%, depending on the packet size and the low station ratio, compared to LCA, on the other hand, the improvement ranges from 16.23% to 27.44% when the comparison is against PFCA. Although SPCA is devised to reduce the system PAoI, the performance is also evaluated in terms of the system AoI which is depicted in Fig. 5.13-b and it shows that SPCA results in lower system AoI compared with the LCA and PFCA for considered scenarios. As shown in 5.13-c, PFCA outperforms the other mechanisms in terms of overall throughput. Although the performance reduction in terms of total throughput for SPCA compared to PFCA ranges from 7.48% to 28.20%, SPCA still provides better performance than LCA in terms of total throughput with the improvement ranging from 17.68% to 41.92% for LSR scenario.

5.7 Optimality Check for SPCA

The proposed model outperforms other models in terms of system PAoI according to the simulation results. However, numerical evidence for the optimality of the SPCA has yet to be presented. We considered a specific simulation environment for the optimality check.

We have considered a network with 2 classes to check the optimal CW_{min} size ratio between two classes. Class 1 consists of stations with the lowest data rate (6 Mbps) and Class 2 consists of stations with the highest data rate (54 Mbps) defined in the 802.11a standard. The simulation parameters for this scenario are shown in Table 5.14.

Table 5.14: Simulation parameters for optimality check

Parameters	**Value**
Packet Size	1472 B
Station Number	32
Station MCS Indices (16 stations from each MCS)	0,7
$CW_{min,i}$ list	$(16, 112, 208, ..., 976)$
Simulation Duration	600 s
Re-transmission limit	7
CW_{max}	1024

A large number of minimum contention window sizes are iterated for stations with two different classes to find the optimal CW_{min} pair that minimizes system PAoI. Before moving on to the simulation results, the expected CW ratio will be stated. When 1472 Byte packet size is used and the encapsulation process is applied as explained in 5.1, the scaling factor of each station with specific MCS is found as given in Table 5.15 for the improved OSP model.

Table 5.15: Contention window scale factors for improved OSP model (1472 Byte)

MCS-7	MCS-6	MCS-5	MCS-4	MCS-3	MCS-2	MCS-1	MCS-0
1.0	1.492	1.984	2.948	3.908	5.763	7.556	8.430

Therefore, we expect that the optimal CW pair should have a CW ratio of $\sqrt{8.430} = 2.903$. Simulation results for this scenario are shown in Fig. 5.14. The

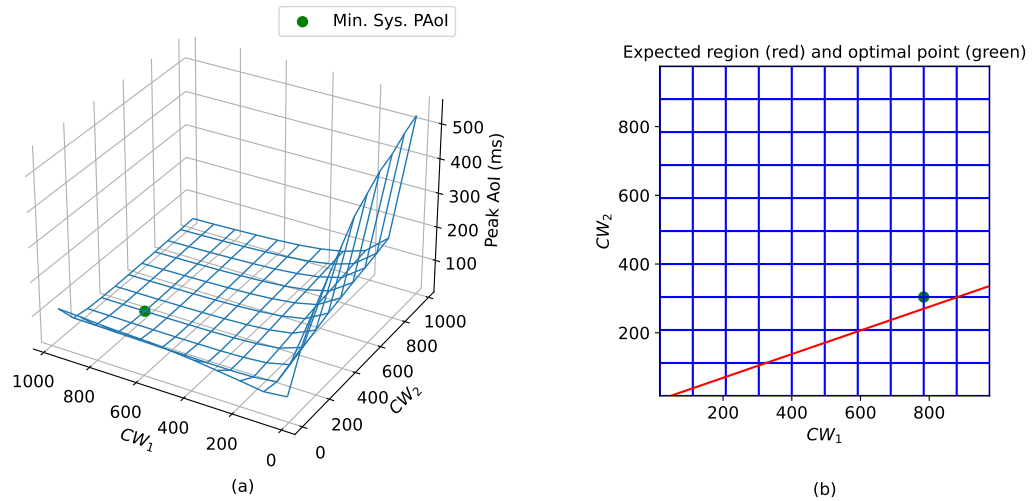

Figure 5.14: Average Peak AoI as a function of CW_1 and CW_2

system PAoI-optimal point is highlighted with green in Fig. 5.14. The optimal point is found when $CW_1 = 784$ and $CW_2 = 304$. As explained previously, the optimal ratio between minimum contention window sizes of the highest and lowest data-rated stations is 2.903 when the packet size is 1472 B. Optimal point has a contention window ratio of 2.578. Our proposed mechanism deviates from the optimal point because of not equal channel utilization parameters. As explained previously, we solved the convex optimization problem in equation (3.8) for a fixed τ. However, when contention windows of stations changed, idle durations, number of collisions change, and channel utilization parameter directly depends on these parameters. Therefore, each CW pair has a different maximum system utilization parameter. In some cases (as in this scenario), higher channel utilization favors some CW pairs. We listed the top 20 CW pairs that minimize system PAoI with their corresponding channel utilization parameters. Results are shown in Table 5.16.

As shown in Table 5.16, our proposed method resulted in third place for this simulation. When we checked the channel utilization parameters of CW pairs

Table 5.16: Top 20 CW pairs that are ordered according to increasing system PAoI

Rank	CW_1	CW_2	CW Ratio	Channel Utilization	System PAoI (ms)
1	784	304	2.578	0.764	39.962
2	976	400	2.440	0.768	39.990
3	880	304	2.895	0.752	40.014
4	688	304	2.263	0.780	40.105
5	880	400	2.2	0.769	40.138
6	976	304	3.210	0.753	40.255
7	784	400	1.960	0.784	40.422
8	592	208	2.846	0.749	40.488
9	592	304	1.947	0.782	40.531
10	496	208	2.384	0.754	40.562
11	976	496	1.967	0.783	40.613
12	688	208	3.307	0.744	40.668
13	688	400	1.720	0.788	41.007
14	880	496	1.774	0.784	41.025
15	784	208	3.769	0.738	41.082
16	400	208	1.923	0.768	41.271
17	496	304	1.631	0.784	41.365
18	976	592	1.648	0.789	41.467
19	880	208	4.230	0.736	41.568
20	784	496	1.581	0.787	41.607

placed as first and second, we observed that they have higher channel utilization than our proposed model. This is an expected result since CW Ratio is lower than our proposed model, which results in more occupation of channel by slow-speed stations. Therefore there are much less ACK messaging and idle time. This observation is observed in the LCA mechanism as well, which resulted in higher channel utilization but LCA cannot outperform SPCA. Higher channel utilization might result in lower system PAoI in some configurations. However, if we reached the same system utilization level, our proposed ratio would be the optimal point. In Fig. 5.14, the deviation of the proposed ratio from the optimal point is %0.092 and 0.037 ms. As a final remark, we observed the last 15 CW pairs. Simulation results for the last 15 CW pairs, ranked from 107 to 121, are shown in Table 5.17.

Table 5.17: Last 15 CW pairs that are ordered according to increasing system PAoI

Rank	CW_1	CW_2	CW Ratio	Channel Utilization	System PAoI (ms)
107	112	592	0.189	0.806	116.836
108	112	688	0.162	0.811	126.438
109	112	784	0.142	0.817	136.610
110	112	880	0.127	0.821	147.193
111	112	976	0.114	0.825	156.428
112	16	112	0.142	0.663	166.311
113	16	208	0.076	0.688	244.386
114	16	304	0.052	0.679	303.114
115	16	400	0.040	0.682	353.837
116	16	496	0.032	0.685	409.006
117	16	592	0.027	0.688	432.521
118	16	688	0.023	0.687	464.113
119	16	784	0.020	0.685	488.852
120	16	880	0.018	0.692	514.124
121	16	976	0.016	0.692	533.179

As shown in Table 5.17, when the CW ratio gets smaller, system PAoI increases drastically. This occurs since the channel access probability of fast stations is decreased and vice versa. Therefore slow stations get the channel frequently and occupy the channel for a long time. In that case, fast stations cannot transmit their status update messages to AP for a long time which results in a large system PAoI. When ranks between 107-111 are investigated, we can see that CW_1 stays constant and CW_2 increases. Since channel access probabilities of fast stations decrease with increasing CW, system PAoI increases. Also, we can see that channel utilization increases as we move from rank 107 to 111. This is again an expected result since the channel access chance of slow stations increases too much and the channel is occupied more by successful transmission. On the other hand, there will be less packet transmissions. When we move from rank 111 to 112, we can observe a drastic decrease in channel utilization. This occurs

since CW_1 is decreased to 16 when there are 16 slow and 16 fast stations in the network. Selection of $CW_1 = 16$ is the worst possible choice since it results in frequent collisions between stations due to the selection of the same number of slots in the backoff stage. We can observe the same trend between ranks 113 and 121, which results in an increase in CW_2 resulting in higher system PAoI. As a final note, rank 111 has higher utilization than the CW pair in the first place, but as seen from the results, higher utilization does not mean better system PAoI. System PAoI is minimized when stations with high service rates are assigned low CW_{min}, and stations with low service rates are assigned with high CW_{min}.

Chapter 6

Conclusion and Future Works

In this thesis, we investigated the system PAoI in a multi-rate CSMA/CA based IEEE 802.11 DCF environment where N stations with a generate-at-will model contend for the channel to transmit their status update messages to the Access Point. By solving a convex optimization problem for system PAoI, we derived channel access probabilities of each source in a multi-rate environment. Implementing a model that adjusts channel access probabilities as in derived expression was a simple task. We have adjusted the CW_{min} parameter of each source such that channel access probabilities are equivalent to derived probabilities. We proposed a channel access mechanism called SPCA to reduce the system PAoI by which the CW_{min} parameters of the stations are chosen to be proportional with the square root of their packet transmission times, as opposed to their packet transmission times, the latter being used in proportional fair channel access mechanisms. Numerical implementation of the proposed method in the IEEE 802.11a network was provided and the performance of the model was evaluated by comparing existing throughput-fair and airtime-fair models in the literature. Our simulation results for considered system configurations reveal that the proposed SPCA scheme leads to a performance improvement in terms of system PAoI up to 12.04% and 27.44% compared to throughput-fair legacy channel access (LCA) and proportional-fair channel access (PFCA), respectively while it

results in throughput reduction compared to PFCA. In this work, for each channel access mechanism, we selected the minimum contention window size for the fastest station, namely $CW_{min,f}$, in an offline manner using simulations so that the system PAoI is minimized. Future work is needed for more efficient and online mechanisms for the choice of $CW_{min,f}$. Also, the proposed SPCA mechanism directly uses a CW_{min} scaling method that is used for providing air-time fairness among stations. However, the accuracy of the air-time fair model decreases as CW_{min} decreases. Therefore, the proposed SPCA mechanism deviates more from the optimal point for the networks with a small number of stations. Therefore, a new model should be proposed in the future to reduce system PAoI for networks with a low number of stations.

Bibliography

[1] "IEEE Standard for Information technology—Telecommunications and information exchange between systems Local and metropolitan area networks—Specific requirements - Part 11: Wireless LAN Medium Access Control (MAC) and Physical Layer (PHY) Specifications," *IEEE Std 802.11-2016 (Revision of IEEE Std 802.11-2012)*, pp. 1–3534, 2016.

[2] S. Kaul, R. Yates, and M. Gruteser, "Real-time status: How often should one update?," in *IEEE INFOCOM*, pp. 2731–2735, 2012.

[3] R. D. Yates, Y. Sun, D. R. Brown, S. K. Kaul, E. Modiano, and S. Ulukus, "Age of information: An introduction and survey," *IEEE Journal on Selected Areas in Communications*, vol. 39, no. 5, pp. 1183–1210, 2021.

[4] A. Kosta, N. Pappas, V. Angelakis, *et al.*, "Age of information: A new concept, metric, and tool," *Foundations and Trends® in Networking*, vol. 12, no. 3, pp. 162–259, 2017.

[5] M. Costa, M. Codreanu, and A. Ephremides, "Age of information with packet management," in *IEEE International Symposium on Information Theory*, pp. 1583–1587, 2014.

[6] N. Akar and E. Karasan, "Is proportional fair scheduling suitable for age-sensitive traffic?," *Computer Networks*, vol. 226, p. 109668, 2023.

[7] M. Heusse, F. Rousseau, G. Berger-Sabbatel, and A. Duda, "Performance anomaly of 802.11b," in *IEEE INFOCOM*, pp. 836–843 vol.2, 2003.

[8] L. B. Jiang and S. C. Liew, "Proportional fairness in wireless lans and ad hoc networks," in *IEEE Wireless Communications and Networking Conference*, vol. 3, pp. 1551–1556 Vol. 3, 2005.

[9] F. Kelly, "Charging and rate control for elastic traffic," *Eur. Trans. Telecommun.*, vol. 8, no. 1, pp. 33–37, 1997.

[10] H. Kim, S. Yun, I. Kang, and S. Bahk, "Resolving 802.11 performance anomalies through qos differentiation," *IEEE Communications Letters*, vol. 9, no. 7, pp. 655–657, 2005.

[11] P. Topor, "DCF-Simpy: A Discrete-Event Simulation Model for IEEE 802.11 DCF Using Simpy," 2021. `https://github.com/ToporPawel/DCF-Simpy`, Accessed on 30.07.2023.

[12] A. M. Bedewy, Y. Sun, S. Kompella, and N. B. Shroff, "Optimal sampling and scheduling for timely status updates in multi-source networks," *IEEE Transactions on Information Theory*, vol. 67, no. 6, pp. 4019–4034, 2021.

[13] I. Kadota, A. Sinha, E. Uysal-Biyikoglu, R. Singh, and E. Modiano, "Scheduling policies for minimizing age of information in broadcast wireless networks," *IEEE/ACM Transactions on Networking*, vol. 26, no. 6, pp. 2637–2650, 2018.

[14] H. Chen, Y. Gu, and S.-C. Liew, "Age-of-information dependent random access for massive iot networks," in *IEEE INFOCOM*, pp. 930–935, 2020.

[15] O. T. Yavascan and E. Uysal, "Analysis of Slotted ALOHA with an age threshold," *IEEE Journal on Selected Areas in Communications*, vol. 39, no. 5, pp. 1456–1470, 2021.

[16] M. Ahmetoglu, O. T. Yavascan, and E. Uysal, "MiSTA: An Age-Optimized Slotted ALOHA Protocol," *IEEE Internet of Things Journal*, vol. 9, no. 17, pp. 15484–15496, 2022.

[17] G. Liva, "Graph-based analysis and optimization of contention resolution diversity slotted aloha," *IEEE Transactions on Communications*, vol. 59, no. 2, pp. 477–487, 2011.

[18] A. Munari, "Modern random access: An age of information perspective on irregular repetition slotted ALOHA," *IEEE Transactions on Communications*, vol. 69, no. 6, pp. 3572–3585, 2021.

[19] Y. Huang, J. Jiao, Y. Wang, X. Zhang, S. Wu, R. Lu, and Q. Zhang, "Age of information minimization for frameless ALOHA in grant-free massive access," *IEEE Transactions on Wireless Communications*, pp. 1–1, 2023.

[20] A. Baiocchi, I. Turcanu, N. Lyamin, K. Sjöberg, and A. Vinel, "Age of Information in IEEE 802.11p," in *IFIP/IEEE International Symposium on Integrated Network Management*, pp. 1024–1031, 2021.

[21] A. Maatouk, M. Assaad, and A. Ephremides, "On the age of information in a csma environment," *IEEE/ACM Transactions on Networking*, vol. 28, no. 2, pp. 818–831, 2020.

[22] J. P. Hespanha, "Modelling and analysis of stochastic hybrid systems," *IEE Proceedings-Control Theory and Applications*, vol. 153, no. 5, pp. 520–535, 2006.

[23] I. Kadota and E. Modiano, "Age of information in random access networks with stochastic arrivals," in *IEEE INFOCOM*, pp. 1–10, 2021.

[24] A. Elgabli, H. Khan, M. Krouka, and M. Bennis, "Reinforcement learning based scheduling algorithm for optimizing age of information in ultra reliable low latency networks," in *IEEE Symposium on Computers and Communications (ISCC)*, pp. 1–6, 2019.

[25] H. B. Beytur and E. Uysal, "Age minimization of multiple flows using reinforcement learning," in *International Conference on Computing, Networking and Communications (ICNC)*, pp. 339–343, 2019.

[26] S. Wang and Y. Cheng, "A deep learning assisted approach for minimizing the age of information in a wifi network," in *IEEE 19th International Conference on Mobile Ad Hoc and Smart Systems (MASS)*, pp. 58–66, 2022.

[27] S. Wang, Y. Cheng, L. X. Cai, and X. Cao, "Minimizing the age of information for monitoring over a wifi network," in *GLOBECOM*, pp. 383–388, 2022.

[28] G. Tan and J. Guttag, "Long-term time-share guarantees are necessary for wireless LANs," in *SIGOPS European Workshop*, 2004.

[29] G. Tan and J. Guttag, "Time-based fairness improves performance in multi-rate WLANs," in *USENIX*, 2004.

[30] B. Li and R. Battiti, "Performance analysis of an enhanced IEEE 802.11 distributed coordination function supporting service differentiation," in *Quality for All, 4th COST 263 International Workshop on Quality of Future, Internet Services, QoFIS 2003, Stockholm, Sweden*.

[31] M. A. Yazici and N. Akar, "Running multiple instances of the distributed coordination function for air-time fairness in multi-rate WLANs," *IEEE Transactions on Communications*, vol. 61, no. 12, pp. 5067–5076, 2013.

[32] M. Heusse, F. Rousseau, R. Guillier, and A. Duda, "Idle sense: An optimal access method for high throughput and fairness in rate diverse wireless LANs," in *Proceedings of Conference on Applications, Technologies, Architectures, and Protocols for Computer Communications*, pp. 121–132, 2005.

[33] T. Joshi, A. Mukherjee, Y. Yoo, and D. P. Agrawal, "Airtime fairness for ieee 802.11 multirate networks," *IEEE Transactions on Mobile Computing*, vol. 7, no. 4, pp. 513–527, 2008.

[34] S. Boyd, S. P. Boyd, and L. Vandenberghe, *Convex optimization*. Cambridge University Press, 2004.

[35] G. Bianchi, "Performance analysis of the IEEE 802.11 distributed coordination function," *IEEE Journal on Selected Areas in Communications*, vol. 18, no. 3, pp. 535–547, 2000.

[36] N.-. D. Team, *ns-3: a discrete-event network simulator*, 2021. `https://www.nsnam.org`, Accessed on 30.07.2023.